Journal of Cerebral Blood Flow & Metabolism (2008), 1–10

www.jcbfm.com

# A physiologic model for recirculation water correction in $CMRO_2$ assessment with $^{15}O_2$ inhalation PET

Nobuyuki Kudomi, Takuya Hayashi, Hiroshi Watabe, Noboru Teramoto, Rishu Piao, Takayuki Ose, Kazuhiro Koshino, Youichirou Ohta and Hidehiro Iida

*Department of Investigative Radiology, Advanced Medical-Engineering Center, National Cardiovascular Center Research Institute, Osaka, Japan*

**Cerebral metabolic rate of oxygen ($CMRO_2$) can be assessed quantitatively using $^{15}O_2$ and positron emission tomography. Determining the arterial input function is considered critical with regards to the separation of the metabolic product of $^{15}O_2$ (RW) from a measured whole blood. A mathematical formula based on physiologic model has been proposed to predict RW. This study was intended to verify the adequacy of that model and a simplified procedure applying that model for wide range of species and physiologic conditions. The formula consists of four parameters, including of a production rate of RW (*k*) corresponding to the total body oxidative metabolism ($BMRO_2$). Experiments were performed on 6 monkeys, 3 pigs, 12 rats, and 231 clinical patients, among which the monkeys were studied at varied physiologic conditions. The formula reproduced the observed RW. Greater *k* values were observed in smaller animals, whereas other parameters did not differ amongst species. The simulation showed $CMRO_2$ sensitive only to *k*, but not to others, suggesting that validity of determination of only *k* from a single blood sample. Also, *k* was correlated with $BMRO_2$, suggesting that *k* can be determined from $BMRO_2$. The present model and simplified procedure can be used to assess $CMRO_2$ for a wide range of conditions and species.**
*Journal of Cerebral Blood Flow & Metabolism* advance online publication, 5 November 2008; doi:10.1038/jcbfm.2008.132

**Keywords:** arterial input; $CMRO_2$; mathematical modeling; recirculation water; PET

## Introduction

Cerebral metabolic rate of oxygen ($CMRO_2$) can be quantitatively assessed using $^{15}O$-labeled oxygen ($^{15}O_2$) and positron emission tomography (PET). This technique is based on an estimation of influx rate of $^{15}O_2$ to the cerebral tissue from arterial blood. Using information of cerebral blood flow (CBF) that may be obtained either from a separate scan with $^{15}O$-labeled water ($H_2^{15}O$) or from the clearance rate $^{15}O_2$ of tissue, the oxygen extraction fraction (OEF) can also be calculated. The arterial input function must be determined before beginning this calculation. More specifically, a metabolic product of $^{15}O_2$ in the arterial blood, as a form of $^{15}O$-labeled water (i.e., recirculating $^{15}O$-water or RW) needs to be accurately estimated.

The arterial whole blood radioactivity curve can be obtained by measuring the radioactivity concentration of continuously withdrawn whole blood using a monitoring device (Eriksson *et al*, 1988; Eriksson and Kanno, 1991; Votaw and Shulman, 1998; Kudomi *et al*, 2003). Assessment of a time-dependent RW curve may be achieved by separating the plasma from the whole blood samples. This, however, requires labor-intensive procedures of frequent, manual arterial blood samplings, the centrifugation of all collected blood samples, and radioactivity measurements for both whole blood and plasma (Holden *et al*, 1988).

Ohta *et al* (1992) proposed to neglect the component of RW from the arterial input function. This technique fits three parameters of $CMRO_2$, CBF, and

Correspondence: Dr H Iida, Department of Investigative Radiology, Advanced Medical-Engineering Center, National Cardiovascular Center Research Institute, 5-7-1, Fujishirodai, Suita, Osaka 565-8565, Japan.
E-mail: iida@ri.ncvc.go.jp
This study was supported by the Program for Promotion of Fundamental Studies in Health Science of the Organization for Pharmaceutical Safety and Research of Japan, a Grant for Research on Advanced Medical Technology from the Ministry of Health, Labour and Welfare (MHLW), Japan, and by Nakatani Electronic Measuring Technology Association of Japan (NK).
Received 2 May 2005; revised 6 October 2008; accepted 11 October 2008

cerebral blood volume (CBV) to the kinetic $^{15}O_2$ data obtained from a single PET scan after the bolus administration of $^{15}O_2$. To minimize errors which result from neglecting RW, only the initial 3 mins of data after the bolus inhalation of $^{15}O_2$ were used when calculating the parameters. This approach has been applied to evaluate the magnitude of increase in $CMRO_2$ relative to that in CBF during cognitive stimulation tasks (Fujita *et al*, 1999; Vafaee and Gjedde, 2000; Okazawa *et al*, 2001*a*, *b*; Yamauchi *et al*, 2003; Mintun *et al*, 2002), but one of the drawbacks to this technique is the lack of accurate statistics, which is due to the use of a short scan duration.

Iida *et al* (1993) have developed a mathematical formula to predict the production of RW based on a physiologic model, which allows prolongation of the PET acquisition period with an additional statistical accuracy. The formula assumes a fixed rate constant for production of RW from $^{15}O_2$ in the body. This is based on the fact that the observed rate constant did not vary among clinical subjects, and thus causes nonsignificant errors in $CMRO_2$. However, the study is limited only to human subjects studied at rest, and results have not been verified using other species such as rat and mouse (Magata *et al*, 2003; Temma *et al*, 2006; Yee *et al*, 2006). Also, the findings have not been evaluated on humans who are under physiologic stress, though under such conditions the whole-body oxygen consumption is expected to change. Moreover, it is important to extend the approach to physiologically stressed conditions as recent progress for assessing $CMRO_2$ and CBF simultaneously from a short period dynamic scan by using a dual tracer autoradiography (DARG) (Kudomi *et al*, 2005). The DARG has enabled the $^{15}O_2$ PET to assess $CMRO_2$ and CBF simultaneously at various physiologically activated conditions.

The aim of this study is to verify the method used to estimate the arterial RW during the $^{15}O_2$ inhalation for simultaneous determination of $CMRO_2$ and CBF from the rapid procedures of $^{15}O_2$ PET. The feasibility of a simplified procedure is also being investigated. Applicability of this approach was tested for a wide range of species under various physiologic conditions. Experiments were designed to apply for different species as well as different physiologic conditions. A simulation study was also performed to evaluate the level of error sensitivity associated with this approach.

## Materials and methods

### Theory

Variables used in the recirculating water model are summarized in Table 1. The mathematical model that formulates the time-dependent RW in arterial blood consists of three rate constants: (1) the production rate of RW or $k$ (per min), proportional to oxidative metabolism in the total body system ($BMRO_2$), (2) the forward diffusion rate ($k_w$, per min) of the metabolized $^{15}O$-water between the blood and interstitial spaces in the body, and (3) the backward diffusion rate ($k_2$, per min) of the metabolized $^{15}O$-water between the blood and interstitial spaces in the body. The differential equations for the arterial activity concentration of $^{15}O$-water at a time $t$ (secs) ($A_w(t)$, Bq/mL), after the physical decay correction can be expressed as follows (Huang *et al*, 1991):

$$\frac{d}{dt}A_w(t) = k \cdot A_o(t) - k_w \cdot A_w(t) + k_2 \cdot C(t) \quad (1a)$$

$$\frac{d}{dt}C(t) = k_w \cdot A_w(t) - k_2 \cdot C(t) \quad (1b)$$

$$A_t(t) = A_o(t) + A_w(t) \quad (1c)$$

where $A_o(t)$ and $A_t(t)$ denote the radioactivity concentration of the arterial $^{15}O_2$ and the total radioactivity from both

**Table 1** Variables used in the recirculating water model

| *Symbol* | *Description* | *Unit* |
|---|---|---|
| $A_o$ | Radioactivity concentration of arterial $^{15}O_2$ | Bq/mL |
| $A_w$ | Radioactivity concentration of arterial $H_2^{15}O$ | Bq/mL |
| $A_t$ | Total radioactivity concentration from arterial $^{15}O_2$ and $H_2^{15}O$ | Bq/mL |
| $A_{plasma}$ | Radioactivity concentration of arterial plasma | Bq/mL |
| $C$ | Activity concentration of $H_2^{15}O$ in peripheral tissue in a body | Bq/mL |
| $Fi_{O_2}$ | Oxygen concentration in inhaled gas | % |
| $Fe_{O_2}$ | Oxygen concentration in expired gas | % |
| $k$ | Production rate of recirculating $H_2^{15}O$ | per min |
| $k_{BM}$ | Production rate of recirculating $H_2^{15}O$ obtained from BM approach | per min |
| $k_w$ | Forward diffusion rate of $H_2^{15}O$ from blood to body interstitial space | per min |
| $k_2$ | Backward diffusion rate of $H_2^{15}O$ from blood to body interstitial space | per min |
| $\lambda$ | Decay constant of $^{15}O$ (=0.00567 per sec) | per sec |
| $v$ | Stroke volume | mL |
| $p$ | $k_w/k_2$ | |
| $r$ | Respiration rate | per min |
| $R$ | Fractional water content ratio in whole blood to that in the plasma | |
| $R_{O_2}$ | Rate of oxidative metabolism in the whole-body system | mL/min |
| $\Delta t$ | Delayed appearance time of recirculating water | secs |
| $V_{O_2}$ | Total volume of molecular oxygen in total blood | mL |
| $V_{TB}$ | Total volume of blood in a body | mL |

$^{15}O_2$ and $H_2^{15}O$, respectively. $C(t)$ is an activity concentration of $H_2^{15}O$ in the peripheral tissue of the total body. Assuming a delayed appearance of RW by $\Delta t$ (Iida *et al*, 1993), the following equation can be obtained:

$$A_w(t+\Delta t) = k(\alpha_1 \cdot A_t(t) \otimes \exp(-\beta_1 t) + \alpha_2 \cdot A_t(t) \otimes \exp(-\beta_2 t)) \quad (2)$$

where $\otimes$ denotes the convolution integral and:

$$\alpha_{1,2} = \frac{a - 2c \pm \sqrt{a^2 - 4b}}{\pm 2\sqrt{a^2 - 4b}}, \quad \beta_{1,2} = \frac{a \pm \sqrt{a^2 - 4b}}{2},$$
$$a = k + k_w + k_w/p, \quad b = k \cdot k_w/p, \quad c = k_w/p, \quad p = k_w/k_2 \quad (3)$$

Following four approaches were performed to determine the rate constants and $A_w(t)$.

*Approach by four parameters fitting*: Four parameters, $k$, $\Delta t$, $k_w$, and $p$ $(=k_w/k_2)$, can be determined from the observed RW $(A_w(t))$ and the $A_t(t)$ curves by means of the nonlinear least square fitting (4PF approach).

*Approach by one parameter fitting*: Once three parameters, $\Delta t$, $k_w$, and $p$, are fixed by averaging values determined by the 4PF approach, $k$ can then be determined by fitting the Equation 2 to measured $A_w(t)$ from $A_t(t)$ (1PF approach). In this procedure, single datum is sufficient, and thus $k$ can be determined from $A_t(t)$ and the RW counts sampled at a single time point.

*Approach from steady-state condition*: Similarly to the 1PF procedures, $k$ can be determined from the steady state condition, which is achieved by a continuous administration of $^{15}O_2$ as follows (SS approach). Incorporating the decay constant of $^{15}O$ ($\lambda = 0.00567$ per secs) into Equations 1a and 1b provides:

$$\frac{d}{dt}A^*_w(t) = k \cdot A^*_o(t) - k_w \cdot A^*_w(t) + k_2 \cdot C^*(t) - \lambda \cdot A^*_w(t) \quad (4a)$$

$$\frac{d}{dt}C^*(t) = k_w \cdot A^*_w(t) - k_2 \cdot C^*(t) - \lambda \cdot C^*(t) \quad (4b)$$

where variables with the symbol * denote that no correction was made for the radioactivity decay of $^{15}O$. After continuously administrating $^{15}O_2$, the radioactivity distribution of $A^*_o(t)$, $A^*_w(t)$, and $C^*_t(t)$ reaches a steady state. Thus, the following equations hold:

$$0 = k \cdot A^*_o(t) - k_w A^*_w(t) + k_2 C^*(t) - \lambda A^*_w(t) \quad (5a)$$

$$0 = k_w A^*_w(t) - k_2 C^*(t) - \lambda C^*(t) \quad (5b)$$

Given the values of $k_w$ and $k_2$ which are determined as averages of 4PF, $k$ can be calculated from the arterial $^{15}O_2$ and $H_2^{15}O$ concentrations at steady state as follows:

$$k = \lambda\left(\frac{k_w + k_2 + \lambda}{k_2 + \lambda}\right)\frac{A^*_w(t)}{A^*_o(t)} \quad (6)$$

*Approach by the rate of whole body oxidative metabolism*: In this study, an alternative approach is provided to obtain $k$, from the rate of oxidative metabolism in the whole-body system (BM approach). With this alternative approach, we assume that the production rate of RW or $k$ is proportional to the rate of oxidative metabolism in the whole-body system (i.e., $BMRO_2$ ($R_{O_2}$, mL/min)). The rate of oxidative metabolism may change dependent on physiologic status of the subject. In addition, we assumed that this index can be defined from the difference of oxygen concentration between inhaled and exhaled trachea air samples. Therefore, the above can be expressed as follows:

$$k = c \cdot \frac{R_{O_2}}{V_{O_2}} \ (\text{per min}) \quad (7a)$$

or

$$k_{BM} = \frac{k}{c} = \frac{R_{O_2}}{1.36 \cdot Hb \cdot V_{TB}} \quad (7b)$$

where $c$ is the proportionality constant, $k_{BM}$ the production rate of RW obtained from BM approach, $V_{O_2}$ (mL) the total volume of molecular oxygen in total blood, 1.36 mL/g the amount of oxygen molecules combined with unit mass of hemoglobin, Hb (g/mL) represents the hemoglobin concentration in the arterial blood, and $V_{TB}$ (mL) is the total volume of blood in the body.

## Simulation

A series of simulation studies were performed to investigate the effects of errors on estimated $CMRO_2$ value in the model parameters ($k$, $\Delta t$, $k_w$, and $p$). In these simulations, a typical arterial blood time activity curve (TAC) of $^{15}O_2$ and $H_2^{15}O$ after DARG protocol (Kudomi *et al*, 2005) obtained in a monkey study was used. RW TACs were generated from the whole blood TAC by assuming baseline values of $k$ as 0.13, 0.11, 0.34, and 0.73 per min, $\Delta t$ as 20, 11, 5, and 3 secs, $k_w$ as 0.38, 0.43, 0.98, and 0.87 per min, and $p$ as 1.31, 1.01, 0.98, and 0.83, corresponding to humans, pigs, monkeys, and rats, respectively. Tissue TACs were generated by assuming CBF = 50 mL/min per 100 g and OEF = 0.4 ($CMRO_2$ was defined as: $CMRO_2 = CBF \times OEF \times C_aO_2$, where $C_aO_2$ is the arterial oxygen content. This simulation was intended to investigate magnitude of error as a percentage difference, so that arbitrary value of $C_aO_2$ was assumed) (Hayashi *et al*, 2003), using a kinetic formula for oxygen and water in the brain tissue (Mintun *et al*, 1984; Shidahara *et al*, 2002; Kudomi *et al*, 2005). $CMRO_2$ values were calculated by the DARG method (Kudomi *et al*, 2005), in which RW TACs were separated from the whole blood by changing $k$ from 0.0 to 1.0 per min, $\Delta t$ from 0 to 30 secs, $k_w$ from 0.0 to 2.0 per min, and $p$ from 0.0 to 2.0, respectively. Errors in the estimated $CMRO_2$ were presented as a percentage difference from the assumed true values.

## Subjects

Subjects consisted of four groups including monkeys, pigs, rats, and clinical patients. Monkeys were six healthy *macaca fascicularis* with body weight of $5.2 \pm 0.8$ kg and age ranging from 3- to 4-year old. Pigs were three farm pigs

with body weight of 38 ± 9 kg and age from 4 to 12 months. Rats were 12 male Wistar rats with body weight of 300 ± 54 g and age from 7 to 8 weeks. All animals were studied during anesthesia. The animals were maintained and handled in accordance with guidelines for animal research on Human Care and Use of Laboratory Animals (Rockville, National Institute of Health/Office for Protection from Research Risks, 1996). The study protocol was approved by the Subcommittee for Laboratory Animal Welfare of National Cardiovascular Center.

Human data were retrospectively sampled from an existing database at National Cardiovascular Center which documented subjects who underwent PET examination after the $^{15}O$-steady-state protocol. There were 231 total samples, with body weight and age ranging from 58 ± 10 kg, and 63 ± 14 years, respectively. Only the arterial $^{15}O_2$ and $H_2^{15}O$ radioactivity concentrations measured at the steady-state condition were used for the present analysis.

## Experimental Protocol

The six monkeys were anesthetized using propofol (4 mg/kg/h) and vecuronium (0.05 mg/kg/h) assigned as a baseline in contrast to the after physiologically stimulated conditions. Animals were intubated and their respiration was controlled by an anesthetic ventilator (Cato, Drager, Germany). Each monkey inhaled 2,200 MBq $^{15}O_2$ for 20 secs. After 3 mins, the monkeys were injected with 370 MBq $H_2^{15}O$ for 30 secs by the anterior tibial vein. This was aimed at assessing both CBF and $CMRO_2$ according to the DARG technique (Kudomi *et al*, 2005). At 30 secs before inhaling $^{15}O_2$ to the monkeys, arterial blood was withdrawn from the femoral artery for 420 secs at a rate of 0.45 mL/min using a Harvard pump (Harvard Apparatus, Holliston, MA, USA). The whole blood TAC was measured with a continuous monitoring system (Kudomi *et al*, 2003) and the $A_t(t)$ was obtained. Meanwhile, we also manually obtained 0.5 mL of arterial blood samples from the contralateral femoral artery at 30, 50, 70, 90, 110, 130, 160, 190, and 360 secs after the $^{15}O_2$ inhalation. For the analysis of sampled blood, 0.2 mL of the blood were used for measurement of the radioactivity concentration of the whole blood, and the rest of the blood sampled (~0.3 mL) was immediately centrifuged for separation to measure the plasma radioactivity concentration ($A_{plasma}(t)$, Bq/mL). The radioactivity concentration was measured using a well counter (Molecular Imaging Laboratory Co. Ltd, Suita, Japan).

In two monkeys, anesthetic level was changed by altering the injection dose of propofol from 4 (baseline) to 8 and then to 12 and 16 mg/kg/h in one monkey, and to 5 and then to 7, 10, and 15 mg/kg/h in the other. In another monkey, $PaCO_2$ level was varied from 39 (baseline) to 47, and then to 33, 26, and 42 mm Hg by changing the respiratory rate. Each measurement for $^{15}O_2$ inhalation and $H_2^{15}O$ injection was initiated after at least 30 mins of applying the physiologic stimulation to achieve a steady state. All procedures were the same as those for the baseline, with the exception of the manual blood sample, which was obtained only once at 70 secs.

Before and after 6 mins of the $^{15}O_2$ inhalation, oxygen concentration in both inhaled ($Fi_{O_2}$, %) and end-tidal expiratory gas ($Fe_{O_2}$, %) was measured by the anesthetic ventilator in five out of the six monkeys. Using the respiration rate ($r$, per min) and the stroke volume ($v$, mL) indicated on the ventilator, the $BMRO_2$ ($R_{O_2}$ mL/min) was calculated using the following equation:

$$R_{O_2} = (Fi_{O_2} - Fe_{O_2}) \cdot v \cdot r.$$

All monkeys received a PET measurement to assess the $CMRO_2$ at physiologically baseline condition. The scan protocol followed the DARG technique (Kudomi *et al*, 2005) in which a 6-mins single dynamic PET scan was performed in conjunction with the administration of dual tracers (i.e., $^{15}O_2$ followed by $H_2^{15}O$ after a 3-mins interval). PET scanner used was ECAT HR (Siemens-CTI, Knoxville, TN, USA), which provided 47 tomographic slice images for an axial field-of-view of approximately 150 mm. We performed arterial–sinus blood sampling to obtain a global OEF ($OEF_{A-V}$) (A–V difference approach). We sampled 0.2 mL of arterial and sinus blood simultaneously during each PET scan and measured their oxygen content ($C_aO_2$ and $C_vO_2$, respectively) (Kudomi *et al*, 2005). The $OEF_{A-V}$ was calculated as: $OEF_{A-V} = (C_aO_2 - C_vO_2)/C_aO_2$.

With regards to the farm pigs involved in this experiment, we used existing data, which were originally obtained in one of the myocardial projects. During the study, three farm pigs were anesthetized. Anesthesia was induced by ketamine (10 mg/kg) and maintained using propofol (4 mg/kg/h). Animals were intubated and their respiration was controlled by the anesthetic ventilator. Venous blood was labeled with $^{15}O_2$ using a small artificial lung unit (Magata *et al*, 2003). $^{15}O_2$-labeled blood (222 to 700 MBq) was injected for 10 secs via anterior tibial vein. At 30 secs before this injection, arterial blood was withdrawn from the femoral artery at a rate of 0.45 mL/min using the Harvard pump and continued for 420 secs. The whole blood TAC ($A_t(t)$) was then measured with a continuous monitoring system (Kudomi *et al*, 2003). Meanwhile, we manually sampled 0.5 mL of arterial blood from the contralateral femoral artery at 30, 60, 90, 90, 120, 180, 240, and 300 secs after the $^{15}O_2$-labeled blood injection. For the analysis of sampled blood, 0.2 mL of the blood were used for measurement of the radioactivity concentration of the whole blood, and the rest of the blood sampled (~0.3 mL) was immediately centrifuged for separation to measure the plasma radioactivity ($A_{plasma}(t)$, Bq/mL). The radioactivity was measured using the well counter.

Data for rats were also originally obtained for other projects, and only the blood counts were used in this study. Anesthesia was induced with pentobarbital (50 mg/kg). A 10 mL of venous blood was labeled $^{15}O_2$ using a small artificial lung unit as described previously (Magata *et al*, 2003), and approximately 1 mL of $^{15}O_2$-labeled blood (37 to 74 MBq) was injected for 30 secs via the tail vein. Arterial blood samples of 0.1 mL each were obtained from the femoral artery at 5-secs intervals for 60 secs and 10-secs intervals for another 60 secs after the injection. Whole blood radioactivity concentration was measured using the well counter to be used as $A_t(t)$. Arterial blood samples of

0.2 mL each were obtained at 30, 60, 90, and 120 secs, and the plasma radioactivity concentration ($A_{plasma}(t)$) was measured by the well counter.

For clinical patients, the blood radioactivity concentration was obtained from previously performed PET examinations, which followed the steady-state protocol (Hirano *et al*, 1994). Each patient inhaled both $^{15}O_2$ and $C^{15}O_2$ to reach the steady state with an inhalation dose of approximately 1,200 and 500 MBq/min, respectively. Five to seven arterial blood samples were obtained during the steady state from the brachial artery. Mean values of radioactivity concentration of the whole blood and plasma, $A_t(t)$ and $A_{plasma}(t)$, respectively, were obtained for both $^{15}O_2$ and $C^{15}O_2$ PET examination.

### Data Analysis

Using the blood activity data obtained from monkeys, pigs, and rats at baseline conditions, $k$ as well as $\Delta t$, $k_w$ and $p$ were first determined by the 4PF approach, in which Equation 2 was applied to fit the $A_w(t)$ using the observed $A_t(t)$. Because the solubility of the oxygen is negligibly small in the plasma, we assumed that all radioactivity in plasma fraction comes from $H_2^{15}O$ and that the water content ratio of whole blood to plasma ($R$) does not change during measurement, which means that the kinetics of water molecules immediately reach equilibrium between the plasma and the cellular fraction (Mintun *et al*, 1984; Iida *et al*, 1993). Thus, $A_w(t)$ was obtained from the equation: $A_w(t) = A_{plasma}(t) \cdot R$, where $R$ value was obtained from the sampled blood at the end of the scan (at which all the radioactivity in the blood can be considered as coming from $H_2^{15}O$ because inhaled $^{15}O_2$ is all metabolized).

Given that the values of $\Delta t$, $k_w$, and $p$ were averages determined from 4PF for monkeys, pigs, and rats, only $k$ was determined by fitting Equation 2 to $A_w$. This was calculated at various points in time, more specifically, in 30, 50, 70, 90, 110, 130, 160, and 190 secs for monkeys, in 30, 60, 90, 90, 120, 180, and 240 secs for pigs, and in 30, 60, 90, and 120 secs for rats. The optimal time point for $k$ under the 1PF approach was determined, so that $(k_{4PF}-k_{1PF})/k_{4PF}$ reaches a minimal value. Here, $k_{4PF}$ and $k_{1PF}$ denote $k$ values determined by the 4PF and 1PF approaches, respectively. The values of $k$ in monkeys at baseline condition, together with those in pigs and rats were compared between 4PF and 1PF approaches, in which a $k$ value from the optimal single time point was used.

In three of the monkeys, which were physiologically stimulated, $k$ of 1PF approach was obtained using single time point of $A_w$. Assuming the total blood volume ($V_{TB}$) for monkeys as 360 mL (Lindstedt and Schaeffer, 2002), and using Hb as measured value in each experiment, $k_{BM}$ was calculated from $R_{O_2}$ according to Equation 7b. Then, $k_{BM}$ obtained as: $k_{BM} = 0.00204R_{O_2}$ was compared with $k$ determined by 1PF.

For clinical data obtained from the steady-state (SS approach) PET examinations, Equation 6 was used to determine the $k$ values of the SS approach for each patient, in which values of $k_w$ and $k_2$ were 0.38 and 0.29 per min as obtained in a previous work by Huang *et al* (1991).

$CMRO_2$ and OEF values in monkeys at baseline condition were calculated using the RW TACs obtained by four different methods (i.e., directly measured $A_w(t)$ ($n = 6$), 4PF ($n = 6$), 1PF ($n = 6$), and BM approaches ($n = 5$)). Regions-of-interest were selected for over the whole brain, and $CMRO_2$ and OEF values were obtained in those regions-of-interest. The $CMRO_2$ values compared among the four methods mentioned above to estimate RW TACs. The Bland–Altman method was applied to analyze the agreement of OEF values between the methods. Also, OEF values were compared with $OEF_{A-V}$.

All data were presented as mean ± 1 standard deviation. Student's $t$-test was used and Pearson's regression analysis was applied to compare two variables. A probability value of $<0.05$ was considered statistically significant.

## Results

Figure 1 shows results from the simulation study, and shows the magnitude of errors in $CMRO_2$ calculated by the DARG method as well as errors in the parameters, $k$, $\Delta t$, $k_w$, and $p$. Errors in $CMRO_2$ were most sensitive to errors in $k$ amongst all species, namely the production rate constant of RW in the arterial blood. After errors in $k$, errors in $CMRO_2$ were sensitive to errors in $\Delta t$. Errors in $k_w$ and $p$, however, appeared to cause relatively insignificant errors in $CMRO_2$. More specifically, only 5 to 10% errors are caused in $CMRO_2$ by a change of ± 50% in $k_w$ and $p$.

Figures 2A–2C show examples of the arterial whole blood curves ($A_t$) and RW TAC ($A_w$) observed in typical studies on a monkey, a pig, and a rat, respectively. The RW curves became constant after a period in all species. The rise time or appearance of the RW curves, $A_w(t)$, was significantly delayed compare to that of whole blood curve, $A_t(t)$. $A_w(t)$ curves fitted by 4PF well reproduced the measured RW curves in three species: monkeys, pigs, and rats. Table 2 summarizes values of $k$, $\Delta t$, $k_w$, and $p$ obtained by the four parameter fitting (4PF approach), at the baseline for monkeys, pigs, and rats, and also $k$ value obtained by the steady-state formula for clinical patients. Those comparisons showed that the $k$ was significantly different among species ($P < 0.001$) except between pig and human subjects, and it was significantly lower in smaller animals. Likewise, $\Delta t$ showed significant differences among the three species ($P < 0.001$), and it was also lower in smaller animals.

Table 3 summarizes $k$ and $CMRO_2$ values obtained from a series of PET experiments performed on six monkeys at baseline condition, and for increased anesthesia (in two monkeys), and changed $PaCO_2$ levels (in one monkey). The best agreement of $k$ values between 4PF and 1PF approaches was obtained from the blood sample data taken at 60, 70, and 60 secs in pigs, monkeys, and rats, respectively, and was used in the 1PF approach. With this

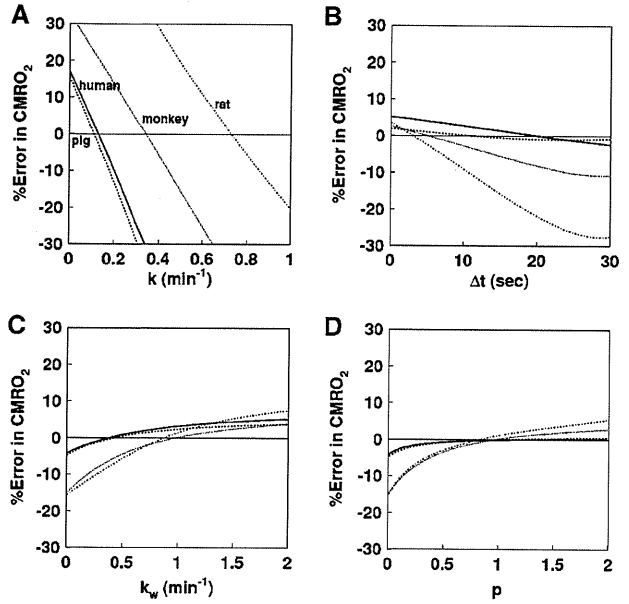


**Figure 1** Error in $CMRO_2$ values due to errors in (**A**) $k$, (**B**) $\Delta t$, (**C**) $k_w$, and (**D**) $p$ for assumed human, pig, monkey and rat. The same type of line indicates the same species. The percentage differences in the $CMRO_2$ values from the assumed true values (Table 1) were plotted as a function of the simulated value of $k$, $\Delta t$, $k_w$, and $p$.

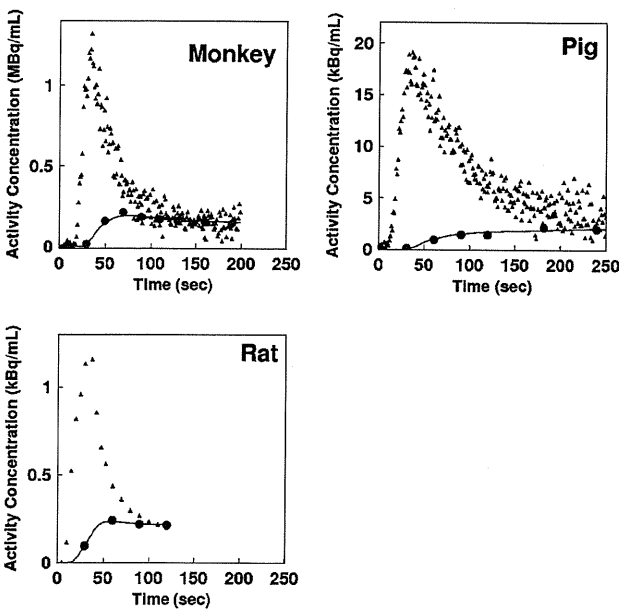


**Figure 2** Representative comparison of the measured arterial whole blood and RW time activity curves for monkey, pig, and rat. Closed triangles and closed circles represent the measured whole blood and RW time activity curves, respectively. Estimated time activity curves by 4PF approach were also plotted in a solid line, and indicated a good agreement with the measured one.

optimized calibration protocol, $k$ values were in a good agreement between 4PF and 1PF approaches. As shown in Figure 3, the regression analysis showed significant correlation for 21 animals including 6 monkeys, 3 pigs, and 12 rats ($P<0.001$), and there was no significant difference between the two variables. Figure 4 shows that $k$ values calculated by the 1PF approach (at an optimized time) were in a good agreement with those calculated with the $BMRO_2$. Namely, the regression analysis showed significant correlation ($P<0.001$, $n=16$) and also that there was no significant difference between the two variables. Note that, in the $CMRO_2$ calculation by $BMRO_2$, $k$ values were normalized according to the regression line shown in Figure 4. It should also be noted that calculated $CMRO_2$ values at the baseline shown in Table 3 were not significantly different among the four techniques. The average ($\pm$s.d.) values of obtained OEF were $0.53 \pm 0.08$, $0.52 \pm 0.09$, $0.54 \pm 0.08$, $0.54 \pm 0.09$, and $0.56 \pm 0.04$ from A–V difference, directly RW measured approach, 4PF, 1PF, and BM approaches, respectively. The Bland–Altman analysis of OEF values between from A–V difference and from others showed small over/underestimation, that is., with bias $\pm$ s.d. of $-0.02 \pm 0.09$, $0.01 \pm 0.07$, $0.01 \pm 0.08$, and $0.02 \pm 0.09$, by direct RW, 4PF, 1PF, and BM approaches, respectively. Neither of the current methods (direct RW, 4PF, 1PF, and BM) was significantly different from A–V difference approach.

## Discussion

Our study showed that the mathematical formula based on the physiologic model that reproduced the time-dependent concentration of RW in the arterial blood after a short-period inhalation of $^{15}O_2$ is indeed adequate. Our approach also simplified the procedures for sequential assessment of RW in $^{15}O_2$ inhalation PET studies, although previous approaches required frequent blood samples and centrifuges of each arterial blood sample. The present approach is an extension of a previous study by Iida *et al* (1993) and Huang *et al* (1991). It is essential if one intends to apply the rapid $^{15}O_2$ PET technique (Kudomi *et al*, 2005) to pharmacologic and physiologic stress studies on a wide range of species. Because the PET acquisition period can be prolonged >3 mins, statistical accuracy can be significantly improved as compared with Ohta *et al* (1992) and other researchers (Fujita *et al*, 1999; Vafaee and Gjedde, 2000; Okazawa *et al*, 2001*a*, *b*; Yamauchi *et al*, 2003; Mintun *et al*, 2002), under which to avoid effects of RW, the data acquisition period was limited only to <3 mins (Meyer *et al*, 1987; Ohta *et al*, 1992).

The present RW formula consists of three rate parameters of the production rate of RW in the arterial blood ($k$), and the forward and backward diffusion rate constants of RW between the blood and the peripheral tissues. The $k$ was presumed to correspond to the oxygen metabolism in the total body system, $BMRO_2$, and was in fact shown to be

**Table 2** Averaged values of $k$, $\Delta t$, $k_w$, and $p$ for monkeys, pigs, rat, and human subjects under baseline condition

| | *Weight (kg)* | k *(per min)* | *Δt (secs)* | *$k_w$ (per min)* | p |
|---|---|---|---|---|---|
| Monkey | $5.2 \pm 0.8^a$ | $0.34 \pm 0.16^a$ | $4.5 \pm 1.4^a$ | $0.98 \pm 0.48$ | $0.98 \pm 0.30$ |
| Pig | $38 \pm 9^a$ | $0.11 \pm 0.02^{a,b}$ | $10.8 \pm 1.8^a$ | $0.83 \pm 0.19$ | $1.01 \pm 0.26$ |
| Rat | $0.30 \pm 0.054^a$ | $0.73 \pm 0.16^a$ | $2.9 \pm 1.7^a$ | $0.87 \pm 0.30$ | $0.83 \pm 0.32$ |
| Human | $58 \pm 10^a$ | $0.129 \pm 0.023^{a,b}$ | — | — | — |

Monkey: $n = 6$; pig: $n = 3$; rat: $n = 12$; and human: $n = 231$. Measured values were obtained by 4PF for monkey, pig, rats, whereas those for human were obtained using data in a steady-state method.

[a]Denotes $P < 0.001$ for other species.

[b]Denotes that the difference was not significant in $k$ between pig and human subjects.

**Table 3** Values of $k$ and $CMRO_2$ in the whole brain region for monkeys under physiologically baseline and stimulated conditions

| *ID* | *Condition* | k *(per min)* | | | *$CMRO_2$ (mL/min per 100 g)* | | | |
|---|---|---|---|---|---|---|---|---|
| | | *4PF* | *1PF* | *$BMRO_2$* | *Reference* | *4PF* | *1PF* | *$BMRO_2$* |
| 1 | BL | 0.36 | 0.42 | — | 3.7 | 3.7 | 3.6 | — |
| 2 | BL | 0.62 | 0.66 | 1.24 | 3.0 | 3.3 | 3.4 | 3.4 |
| 3 | BL | 0.32 | 0.39 | 0.83 | 3.0 | 3.1 | 3.0 | 2.9 |
| | (Dose of propofol) | | | | | | | |
| 4 | BL | 0.21 | 0.18 | 0.55 | 2.0 | 2.0 | 2.0 | 1.8 |
| | 8 mg/kg/h | — | 0.30 | 0.69 | — | — | — | — |
| | 12 mg/kg/h | — | 0.23 | 0.52 | — | — | — | — |
| | 16 mg/kg/h | — | 0.16 | 0.40 | — | — | — | — |
| 5 | BL | 0.12 | 0.15 | 0.31 | 2.1 | 2.1 | 2.0 | 1.8 |
| | 5 mg/kg/h | — | 0.15 | 0.32 | — | — | — | — |
| | 7 mg/kg/h | — | 0.16 | 0.35 | — | — | — | — |
| | 10 mg/kg/h | — | 0.18 | 0.36 | — | — | — | — |
| | 15 mg/kg/h | — | 0.071 | 0.29 | — | — | — | — |
| | ($PaCO_2$ level) | | | | | | | |
| 6 | BL | 0.43 | 0.46 | 0.95 | 2.8 | 3.1 | 3.0 | 3.3 |
| | 47 mm Hg | — | 0.20 | 0.64 | — | — | — | — |
| | 33 mm Hg | — | 0.21 | 0.46 | — | — | — | — |
| | 26 mm Hg | — | 0.14 | 0.28 | — | — | — | — |
| | 42 mm Hg | — | 0.33 | 0.82 | — | — | — | — |

4PF, four parameters fitting; 1PF, one parameter fitting; $BMRO_2$, total body metabolic rate of oxygen; BL, baseline condition.
Reference: RW TAC was obtained using measured RW data at a baseline condition in all monkeys ($n = 6$). No statistically significant differences were found in $CMRO_2$ between reference and other techniques.

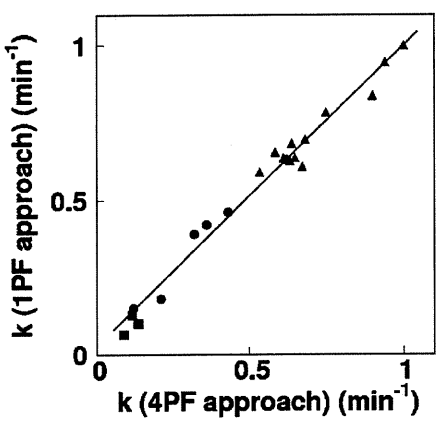


**Figure 3** Comparison of the production rates of RW ($k$, per min) obtained by 4PF and those by 1PF. Squares, circles, and triangles correspond to pigs, monkeys, and rats, respectively. The regression line was $y = 0.97x + 0.026$ (per min) ($r = 0.98$).

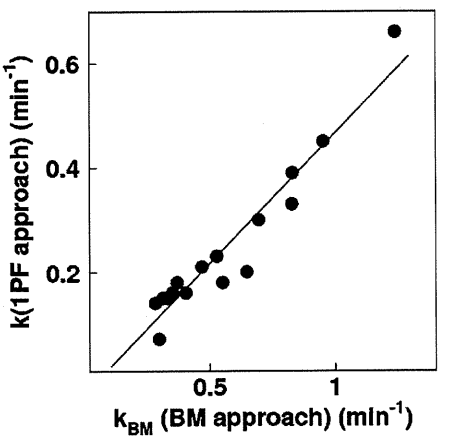


**Figure 4** Comparison of the production rates of RW obtained by BM approach and those by 1PF approach in five monkeys at various anesthetic and $PaCO_2$ levels. The regression line was $y = 0.50x - 0.034$ (per min) ($r = 0.95$).

significantly correlated to $BMRO_2$, as measured from the trachea gas sampling (Figure 4). The latter two parameters ($k_w$ and $p$) appeared to be consistent and did not differ across various species (Table 2). Also, change in those parameters was less sensitive in $CMRO_2$ (Figure 1). These findings suggest that the production of RW after inhalation of $^{15}O_2$ could be described only by a single parameter of $k$, as shown in Figure 3, although further studies are required to validate this because the method was only tested in a group with small number of subjects of particular physiologic situation (under anesthesia) and has not been applied to different populations. It is also important to note that this parameter ($k$) estimated from the $BMRO_2$ (i.e., BM approach) provided $CMRO_2$, which was consistent with the trachea gas samplings shown in Figure 4, and that the obtained OEF values by the approaches of 4PF, 1PF, and BM applied in the present study were not significantly different to that by A–V difference approach as revealed by Bland–Altman analysis.

The simulation study also showed that the most sensitive parameter in $CMRO_2$ was the RW production rate constant, $k$, followed by $\Delta t$. It was therefore suggested that $k$ could be determined with a single blood sampling procedure using the 1PF approach, in which other parameter values were determined and fixed from results from the 4PF approach. It was further showed that $k$ could be obtained from the BM approach as determined from oxygen concentration in the expiration gas. Both 1PF and BM approaches appeared to be robustly useful in $^{15}O_2$ PET for assessing quantitative $CMRO_2$ and CBF in clinical studies.

It is important to note that $k$ varies significantly depending on the physiologic status even in the same species, as seen in Figure 4. According to the simulation study in Figure 1, this variation causes nonnegligible errors in $CMRO_2$, if a constant $k$ is used. Changes in $k$ from 0.1 to 0.6 per min causes errors in $CMRO_2$ of $\pm 30\%$ in anesthetized monkeys. Results from clinical studies, however, showed the variation in $k$ being less. As shown in Table 2, $k$ for clinical patients was $0.129 \pm 0.023$ per min, and the coefficient of variation was approximately 18%. Previous work by Huang *et al* (1991) also showed similar value with comparable variations, namely $0.131 \pm 0.026$ per min in six human subjects. These variations caused only $\pm 5\%$ errors in $CMRO_2$, according to the simulation shown in Figure 1. The small variation in $k$ in clinical patients is attributed to the fact that all subjects were studied at a relatively stable condition without physiologic stimulation. However, careful attention is needed if one intends to scan the patients whose whole-body oxygen metabolism is largely changed from the baseline condition. For example, during several pharmacologically stressed (Wessen *et al*, 1997; Kaisti *et al*, 2003), exercise-induced physically stressed, and hyper- or hypothermia (Sakoh and Gjedde, 2003) conditions.

The simulation also showed that size of errors in $CMRO_2$ increased in smaller animals, where the value of $k$ was larger. Recently, $CMRO_2$ as well as CBF have been measured in rats using a small animal PET scanner (Magata *et al*, 2003; Yee *et al*, 2006). Magata *et al* performed multiple blood samplings and plasma separation for multiple blood samples to estimate the RW in their experiment involving rats. The procedures were crucial, but have caused serious alterations of physiologic condition in heart pressure and heart rate due to large amount of blood samples for small animals. Our proposed simplified technique for estimating RW from a single blood sample or from $BMRO_2$, is essential for small animals to be able to maintain the physiologic status. The calculation of $CMRO_2$ also requires whole blood arterial TAC, which can be obtained from arterial blood samplings and could change the physiologic condition. However, such blood sampling could also be avoided by an arterial–venous bypass (Weber *et al*, 2002; Laforest *et al*, 2005), by placing a probe in femoral artery (Pain *et al*, 2004), or by a noninvasive method (Yee *et al*, 2006).

Mintun *et al* (1984) has proposed a simple procedure for RW correction based on a linear interpolation for the bolus $^{15}O_2$ inhalation 60-secs PET scan. As shown in Figure 2, the RW curve is not linear particularly in smaller animals, and a systematic error may be caused or scan duration is limited. Ohta *et al* (1992) and other investigators (Ohta *et al*, 1992; Fujita *et al*, 1999; Vafaee and Gjedde, 2000; Okazawa *et al*, 2001*a*, *b*; Yamauchi *et al*, 2003; Mintun *et al*, 2002), however, have used a technique which does not take into account the RW contribution. Only initial short-period data, namely the 3 mins after the bolus inhalation of $^{15}O_2$, were used in their approach, and thus estimated parameters suffered from statistical uncertainties. The present methodology to estimate RW in the arterial blood allows the prolongation of a PET acquisition period. The technique can also be applicable to the recently proposed sequential administration protocol of $^{15}O_2$ followed by $H_2^{15}O$ to estimate $CMRO_2$ and CBF simultaneously from a single session of a PET scan (Kudomi *et al*, 2005). This protocol, however, required a separation of a RW TAC from the whole blood TAC as showed recently (Kudomi *et al*, 2007).

The $k_{BM}$ determined from the total body oxygen metabolism, namely the BM approach, was significantly greater than $k$ obtained by the 4PF or the 1PF approach, by a factor 2, as shown in Figure 4. The reason is not clear, but partly attributed to the limitation of the simplified model. The body system consists of various organs which have different oxygen metabolism along with different circulation systems and with transit times. It is well known that the apparent rate constant defined with a simplified compartmental model could be underestimated as compared with an average of true rate constants, known as heterogeneity effects (Iida *et al*, 1989; Aston *et al*, 2002). This is, however, not essential.

Simply, linear correction could be applied to convert to the apparent $k$ value as has been performed in this study. $CMRO_2$ values calculated using BM approach for the RW separation, were in good agreement with those determined with the direct measurement of RW as shown in Table 3.

The current method with modeling approach and simplified procedure provided consistent results in terms of time-dependent RW component, and consequently metabolic product of $^{15}O_2$ was separated from arterial whole blood for the $CMRO_2$ assessment in PET examination. The modeling approach to separate metabolite from authentic tracer has been showed previously for 6-[$^{18}$F]fluoro-L-dopa study (fdopa) (Huang *et al*, 1991). We expect that the modeling approach in conjunction with the simplified method showed in our study could be applied for various kinds of tracers, which require the separation of metabolic product such as fdopa. This approach enables us to assess parametric images for those tracers by eliminating the laborious procedures and by avoiding the amount of blood samplings, particularly for smaller animals.

In conclusion, the present RW model was feasible to reproduce RW TAC from a whole radioactivity concentration curve obtained after $^{15}O_2$ inhalation, and for a wide range of species. The simplified procedure to predict the RW TAC is of use to calculate $CMRO_2$ in smaller animals as well as clinical patients.

## Acknowledgements

We acknowledge Mr N Ejima for operating the cyclotron and daily maintenance of CTI ECAT HR. We also gratefully thank Ms Atra Ardekani for her invaluable help on preparing the present paper. We also thank the staff of the Investigative Radiology, Research Institute, National Cardiovascular Center, especially, Dr T Inomata, Dr H Jino, Dr N Kawachi, and Dr T Zeniya for their assistance.

## References

Aston JA, Cunningham VJ, Asselin MC, Hammers A, Evans AC, Gunn RN (2002) Positron emission tomography partial volume correction: estimation and algorithms. *J Cereb Blood Flow Metab* 22:1019–34

Eriksson L, Holte S, Bohm Chr, Kesselberg M, Hovander B (1988) Automated blood sampling system for positron emission tomography. *IEEE Trans Nucl Sci* 35:703–7

Eriksson L, Kanno I (1991) Blood sampling devices and measurements. *Med Prog Technol* 17:249–57

Fujita H, Kuwabara H, Reutens DC, Gjedde A (1999) Oxygen consumption of cerebral cortex fails to increase during continued vibrotactile stimulation. *J Cereb Blood Flow Metab* 19:266–71

Hayashi T, Watabe H, Kudomi N, Kim KM, Enmi J, Hayashida K, Iida H (2003) A theoretical model of oxygen delivery and metabolism for physiologic interpretation of quantitative cerebral blood flow and metabolic rate of oxygen. *J Cereb Blood Flow Metab* 23:1314–23

Hirano T, Minematsu K, Hasegawa Y, Tanaka Y, Hayashida K, Yamaguchi T (1994) Acetazolamide reactivity on $^{123}$I-IMP single photon emission computed tomography in patients with major cerebral artery occlusive disease: correlation with positron emission tomography parameters. *J Cereb Blood Flow Metab* 14:763–70

Holden JE, Eriksson L, Roland PE, Stone-Elander S, Widen L, Kesselberg M (1988) Direct comparison of single-scan autoradiographic with multiple-scan least-squares fitting approaches to PET $CMRO_2$ estimation. *J Cereb Blood Flow Metab* 8:671–80

Huang SC, Barrio JR, Yu DC, Chen B, Grafton S, Melega WP, Hoffman JM, Satyamurthy N, Mazziotta JC, Phelps ME (1991) Modelling approach for separating blood time-activity curves in positron emission tomographic studies. *Phys Med Biol* 36:749–61

Iida H, Jones T, Miura S (1993) Modeling approach to eliminate the need to separate arterial plasma in oxygen-15 inhalation positron emission tomography. *J Nucl Med* 34:1333–40

Iida H, Kanno I, Miura S, Murakami M, Takahashi K, Uemura K (1989) A determination of the regional brain/blood partition coefficient of water using dynamic positron emission tomography. *J Cereb Blood Flow Metab* 9:874–85

Kaisti KK, Langsjo JW, Aalto S, Oikonen V, Sipila H, Teras M, Hinkka S, Metsahonkala L, Scheinin H (2003) Effects of sevoflurane, propofol, and adjunct nitrous oxide on regional cerebral blood flow, oxygen consumption, and blood volume in humans. *Anesthesiology* 99:603–13

Kudomi N, Choi C, Watabe H, Kim KM, Shidahara M, Ogawa M, Teramoto N, Sakamoto E, Iida H (2003) Development of a GSO detector assembly for a continuous blood sampling system. *IEEE Trans Nucl Sci* 50:70–3

Kudomi N, Hayashi T, Teramoto N, Watabe H, Kawachi N, Ohta Y, Kim KM, Iida H (2005) Rapid quantitative measurement of $CMRO_2$ and CBF by dual administration of $^{15}$O-labeled oxygen and water during a single PET scan—a validation study and error analysis in anesthetized monkeys. *J Cereb Blood Flow Metab* 25:1209–24

Kudomi N, Watabe H, Hayashi T, Iida H (2007) Separation of input function for rapid measurement of quantitative $CMRO_2$ and CBF in a single PET scan with a dual tracer administration method. *Phys Med Biol* 52: 1893–908

Laforest R, Sharp TL, Engelbach JA, Fettig NM, Herrero P, Kim J, Lewis JS, Rowland DJ, Tai YC, Welch MJ (2005) Measurement of input functions in rodents: challenges and solutions. *Nucl Med Biol* 32:679–85

Lindstedt L, Schaeffer PJ (2002) Use of allometry in predicting anatomical and physiological parameters of mammals. *Lab Anim* 36:1–19

Magata Y, Temma T, Iida H, Ogawa M, Mukai T, Iida Y, Morimoto T, Konishi J, Saji H (2003) Development of injectable O-15 oxygen and estimation of rat OEF. *J Cereb Blood Flow Metab* 23:671–6

Meyer E, Tyler JL, Thompson CJ, Redies C, Diksic M, Hakim AM (1987) Estimation of cerebral oxygen utilization rate by single-bolus 15O2 inhalation and dynamic positron emission tomography. *J Cereb Blood Flow Metab* 7:403–14

Mintun MA, Raichle ME, Martin WR, Herscovitch P (1984) Brain oxygen utilization measured with O-15 radio-

tracers and positron emission tomography. *J Nucl Med* 25:177–87

Mintun MA, Vlassenko AG, Shulman GL, Snyder AZ (2002) Time-related increase of oxygen utilization in continuously activated human visual cortex. *Neuroimage* 16:531–7

Ohta S, Meyer E, Thompson CJ, Gjedde A (1992) Oxygen consumption of the living human brain measured after a single inhalation of positron emitting oxygen. *J Cereb Blood Flow Metab* 12:179–92

Okazawa H, Yamauchi H, Sugimoto K, Takahashi M, Toyoda H, Kishibe Y, Shio H (2001*a*) Quantitative comparison of the bolus and steady-state methods for measurement of cerebral perfusion and oxygen metabolism: positron emission tomography study using 15O-gas and water. *J Cereb Blood Flow Metab* 21:793–803

Okazawa H, Yamauchi H, Sugimoto K, Toyoda H, Kishibe Y, Takahashi M (2001*b*) Effects of acetazolamide on cerebral blood flow, blood volume, and oxygen metabolism: a positron emission tomography study with healthy volunteers. *J Cereb Blood Flow Metab* 21:1472–9

Pain F, Laniece P, Mastrippolito R, Gervais P, Hantraye P, Besret L (2004) Arterial input function measurement without blood sampling using a beta-microprobe in rats. *J Nucl Med* 45:1577–82

Sakoh M, Gjedde A (2003) Neuroprotection in hypothermia linked to redistribution of oxygen in brain. *Am J Physiol Heart Circ Physiol* 285:H17–25

Shidahara M, Watabe H, Kim KM, Oka H, Sago M, Hayashi T, Miyake Y, Ishida Y, Hayashida K, Nakamura T, Iida H (2002) Evaluation of a commercial PET tomograph-based system for the quantitative assessment of rCBF, rOEF and rCMRO2 by using sequential administration of 15O-labeled compounds. *Ann Nucl Med* 16:317–27

Temma T, Magata Y, Kuge Y, Shimonaka S, Sano K, Katada Y, Kawashima H, Mukai T, Watabe H, Iida H, Saji H (2006) Estimation of oxygen metabolism in a rat model of permanent ischemia using positron emission tomography with injectable $^{15}O$-$O_2$. *J Cereb Blood Flow Metab* 26:1577–83

Vafaee MS, Gjedde A (2000) Model of blood-brain transfer of oxygen explains nonlinear flow-metabolism coupling during stimulation of visual cortex. *J Cereb Blood Flow Metab* 20:747–54

Votaw JR, Shulman SD (1998) Performance evaluation of the Pico-Count flow-through detector for use in cerebral blood flow PET studies. *J Nucl Med* 39:509–15

Weber B, Burger C, Biro P, Buck A (2002) A femoral arteriovenous shunt facilitates arterial whole blood sampling in animals. *Eur J Nucl Med Mol Imaging* 29: 319–23

Wessen A, Widman M, Andersson J, Hartvig P, Valind S, Hetta J, Langstrom B (1997) A positron emission tomography study of cerebral blood flow and oxygen metabolism in healthy male volunteers anaesthetized with eltanolone. *Acta Anaesthesiol Scand* 41:1204–12

Yamauchi H, Okazawa H, Kishibe Y, Sugimoto K, Takahashi M (2003) The effect of acetazolamide on the changes of cerebral blood flow and oxygen metabolism during visual stimulation. *Neuroimage* 20:543–9

Yee SH, Lee K, Jerabek PA, Fox PT (2006) Quantitative measurement of oxygen metabolic rate in the rat brain using microPET imaging of briefly inhaled 15O-labelled oxygen gas. *Nucl Med Commun* 27:573–81

NeuroImage 47 (2009) 1639–1648

Contents lists available at ScienceDirect

NeuroImage

journal homepage: www.elsevier.com/locate/ynimg

# Quantitative evaluation of changes in binding potential with a simplified reference tissue model and multiple injections of [$^{11}$C]raclopride

Yoko Ikoma [a,b,*], Hiroshi Watabe [a], Takuya Hayashi [a], Yoshinori Miyake [c], Noboru Teramoto [a], Kotaro Minato [b], Hidehiro Iida [a]

[a] Department of Investigative Radiology, National Cardiovascular Center Research Institute, Suita, Osaka, Japan
[b] Graduate School of Information Science, Nara Institute of Science and Technology, Ikoma, Nara, Japan
[c] Department of Radiology and Nuclear Medicine, National Cardiovascular Center Hospital, Suita, Osaka, Japan

ARTICLE INFO

*Article history:*
Received 20 February 2009
Revised 27 May 2009
Accepted 29 May 2009
Available online 9 June 2009

*Keywords:*
Positron emission tomography
[$^{11}$C]raclopride
Dopamine $D_2$ receptor
Multiple injections
Binding potential

ABSTRACT

Positron emission tomography (PET) with [$^{11}$C]raclopride is widely used to investigate temporal changes in the dopamine $D_2$ receptor system attributed to the dopamine release. The simplified reference tissue model (SRTM) can be used to determine the binding potential ($BP_{ND}$) value using the time–activity curve (TAC) of the reference region as input function. However, in assessing temporal changes in $BP_{ND}$ using the SRTM, multiple [$^{11}$C]raclopride PET scans are required, and a second scan must be performed after the disappearance of the [$^{11}$C]raclopride administered in the first scan. In this study, we have developed an extended multiple-injection SRTM to estimate the $BP_{ND}$ change, from a single PET scan with multiple injections of [$^{11}$C]raclopride, and we have validated this approach by performing numerous simulations and studies on monkeys. In the computer simulations, TACs were generated for dual injections of [$^{11}$C]raclopride, in which binding conditions changed during the scans, and the $BP_{ND}$ values before, and after, the second injection were estimated by the proposed method. As a result, the reduction in $BP_{ND}$ was correlated, either with the integral of released dopamine, or with the administered mass of raclopride. This method was applied to studies on monkeys, and was capable of determining two identical $BP_{ND}$ values when there were no changes in binding conditions. The $BP_{ND}$ after the second injection decreased when binding conditions changed due to an increase in administered raclopride. An advantage of the proposed method is the shortened scan period for the quantitative assessment of the $BP_{ND}$ change for neurotransmitter competition studies.



## Introduction

Neuroreceptor imaging using positron emission tomography (PET) and [$^{11}$C]raclopride has made it possible to determine the density of striatal dopamine $D_2$ receptors *in vivo* (Farde et al., 1985; Köhler et al., 1985; Hall et al., 1988). The binding potential ($BP_{ND} = k_3/k_4$) derived from rate constants in a two-tissue compartment model has been used to quantify the receptor binding (Mintun et al., 1984). Endres et al. then developed an extended compartment model, which included the released neurotransmitter concentration, and demonstrated that [$^{11}$C]raclopride binding decreased after the administration of amphetamine, which resulted in the displacement of the raclopride due to competition with increased dopamine (Endres et al., 1997, Carson et al., 1997). The model showed that the change in $BP_{ND}$ between the baseline and the stimulated state was related to the total amount of released dopamine. Applying this theory, it has been shown that amphetamine-related reductions in [$^{11}$C]raclopride-specific binding in patients with schizophrenia was significantly greater than in healthy volunteers (Breier et al., 1997) and that a reduction in [$^{11}$C] raclopride binding was observed while playing a video game which resulted in the release of endogenous dopamine (Koepp et al., 1998). In this competition paradigm, two PET studies are necessary to measure the $BP_{ND}$ values of the baseline and competed conditions, and a long study period is required.

On the other hand, single-scan studies with bolus-plus-continuous infusion (B/I) of the tracer, applied for the measurement of reduction in $BP_{ND}$ due to an amphetamine challenge, were also performed (Carson et al., 1997, Endres et al., 1997). In these studies, a stimulus was administered during infusion of the tracer, and the change in binding between pre- and post-amphetamine intervention was measured as the tissue-to-plasma concentration ratio at equilibrium. This method enables the direct measurement of receptor-binding

* Corresponding author. Department of Investigative Radiology, National Cardiovascular Center Research Institute, 5-7-1, Fujishirodai, Suita, Osaka, 565-8565, Japan. Fax: +81 6 6835 5429.
*E-mail address:* ikoma@ri.ncvc.go.jp (Y. Ikoma).

1053-8119/$ – see front matter © 2009 Elsevier Inc. All rights reserved.
doi:10.1016/j.neuroimage.2009.05.099

changes in a single scan. However, the design of the protocol requires that the tracer kinetics attain equilibrium within the measurement period of the pre- and post-amphetamine challenges (Watabe et al., 2000), and dynamic data that does not reach equilibrium may cause systematic errors in the estimates of binding changes (Zhou et al., 2006).

To compute the $BP_{ND}$ value, the simplified reference tissue model (SRTM) is often used. The SRTM can provide the $BP_{ND}$ without invasive arterial blood sampling by using a time–activity curve (TAC) of the reference region where specific bindings are negligible (Lammertsma and Hume, 1996). Recently, an extended simplified reference tissue model (ESRTM) was developed in order to quantify the reduction in $BP_{ND}$ with B/I administration (Zhou et al., 2006). In the ESRTM method, the $BP_{ND}$ of the SRTM was estimated separately, before and after, the pharmacological challenge during a 90 min scan with B/I administration. The group reported that stimulus-induced $BP_{ND}$ changes, obtained from equilibrium analysis in the non-equilibrium state, resulted in an underestimation of the reduction in $BP_{ND}$, and that this was significantly improved by using the ESRTM. Nonetheless, B/I administration requires the equipment to provide [$^{11}$C]raclopride constantly during the scan, and there are often technical problems.

Kim et al. (2006) developed a method to measure regional cerebral blood flow in pre- and post-pharmacological stress from a single session of single photon emission computed tomography (SPECT) scanning with dual injections of $^{123}$I-iodoamphetamine. In their paper, they showed mathematical derivation for estimating CBF values from two conditions in a single session of SPECT study. By advancing their method, we have developed a method to detect changes in receptor binding using a single session of PET scanning in conjunction with multiple bolus injections of [$^{11}$C]raclopride synthesized once before the scan (Watabe et al., 2006). In our approach, the SRTM was extended to measure the $BP_{ND}$ of each injection, and we validated this approach by performing numerous simulations and studies on monkeys using PET and [$^{11}$C]raclopride.

## Methods

### *Theory*

The simplified reference tissue model (SRTM) provides $BP_{ND}$ without arterial blood sampling by eliminating the arterial plasma TAC arithmetically from model equations, by using the TAC of the reference region where specific bindings are negligible. The radioactivity concentration of the target region ($C_t$) is expressed as Eq. (1), using the radioactivity concentration in the reference region ($C_r$), under the assumption that the target and reference regions can be expressed using the one-tissue compartment model and that the ratios of $K_1$ and $k_2$ are equal between the target and reference regions (Lammertsma and Hume, 1996).

$$C_t(t) = R_1 C_r(t) + \left(k_2 - \frac{R_1 k_2}{1 + BP_{ND}}\right) e^{-\frac{k_2}{1+BP_{ND}}t} \otimes C_r(t) \quad R_1 = K_1 / K_1^r \tag{1}$$

where $K_1$ and $k_2$ are the rate constants for the transfer from plasma to the displaceable compartment in the target tissue and from the displaceable compartment to plasma, respectively, and $K_1^r$ is the rate constant for the transfer from plasma to the reference tissue.

We have extended this SRTM to a multiple-injection study. In this approach, the first injection of the radioligand was performed at the time of the scan start, and the $BP_{ND}$ was measured as a baseline. Next, a second injection was performed simultaneously with a change in binding conditions, and the $BP_{ND}$ was measured as a competitive state after the second injection. The $BP_{ND}$ values before, and after, the second injection, were estimated by the multiple-injection simplified reference tissue model (MI-SRTM) expressed as follows:

$$\begin{aligned} C_{t1}(t) &= R_{11} C_{r1}(t) + \left(k_{21} - \frac{R_{11} k_{21}}{1 + BP_{ND1}}\right) e^{-\frac{k_{21}}{1+BP_{ND1}}t} \otimes C_{r1}(t) \\ C_{t2}(t) &= R_{12} C_{r2}(t) + \left(k_{22} - \frac{R_{12} k_{22}}{1 + BP_{ND2}}\right) e^{-\frac{k_{22}}{1+BP_{ND2}}t} \otimes C_{r2}(t) \\ &\quad + (C_{t0} - R_{12} C_{r0}) e^{-\frac{k_{22}}{1+BP_{ND2}}t} \end{aligned} \tag{2}$$

where $C_{t1}$ and $C_{t2}$ are the radioactivity concentrations in the target tissue and $C_{r1}$ and $C_{r2}$ are the radioactivity concentrations in the reference tissue for the first and second injections, respectively; $t$ is the time from the first or second injection; $C_{t0}$ and $C_{r0}$ are the radioactivity concentrations of the target and reference tissues at the time of the second injection, respectively.

Firstly, $R_{11}$, $k_{21}$ and $BP_{ND1}$ were estimated by nonlinear least squares fitting with the iteration of the Gauss–Newton algorithm using data points before the second injection. Next, $C_{r0}$ was calculated by the interpolation of the measured reference TAC, and $C_{t0}$ was estimated using Eq. (1) with estimated $R_{11}$, $k_{21}$ and $BP_{ND1}$ values. Finally, $R_{12}$, $k_{22}$, and $BP_{ND2}$ were estimated by nonlinear least squares fitting using these $C_{r0}$ and $C_{t0}$ values with Eq. (2). In this study using [$^{11}$C]raclopride, the TAC of the cerebellum was used as a reference TAC.

The present method can be used to generate voxel-based parametric maps. In the voxel-based estimation for parametric imaging of ligand–receptor binding, $R_{11}$, $k_{21}$ and $BP_{ND1}$ from the first injection and $R_{12}$, $k_{22}$, and $BP_{ND2}$ from the second injection in Eq. (2), were estimated by a basis function method in which the model Eq. (2) is solved using linear least squares for a set of basis functions, which enables the incorporation of parameter bounds (Gunn et al., 1997).

### *Simulation analysis*

Three simulation studies were carried out to validate the present approach and to determine: 1) whether the change in $BP_{ND}$ caused by competition to receptor binding could be detected by the MI-SRTM; 2) how would the time delay between the endogenous dopamine release and [$^{11}$C]raclopride injection affect $BP_{ND}$ estimates, and 3) what was an optimal scan duration for a reliable $BP_{ND}$ estimation?

#### *Detection of $BP_{ND}$ change with dual injections*

The MI-SRTM assumes that $BP_{ND}$ alters promptly from $BP_{ND1}$ to $BP_{ND2}$ at the time of the second injection and then remains constant. However, in reality this is unlikely and the binding condition of [$^{11}$C]raclopride may be continuously changed along time. In this simulation, the detectability of the reduction of $BP_{ND}$ due to changes in binding conditions was investigated. Noiseless time–activity curves of the striatum and cerebellum were generated with a measured plasma TAC and assumed parameter values derived from measurements taken from the monkey study. A TAC of the cerebellum was simulated with a conventional two-tissue compartment, four-parameter model with assumed parameter values obtained previously in our monkey study: $K_1 = 0.034$, $K_1/k_2 = 0.36$, $k_3 = 0.022$, $k_4 = 0.034$. Meanwhile, a TAC of the striatum was simulated with an extended two-tissue compartment model

expressed as Eq. (3) by the fourth-order Runge–Kutta method (Endres et al., 1997).

$$\begin{aligned}
\frac{dC_f}{dt} &= K_1 C_p(t) - (k_2 + k'_3(t))C_f(t) + k_4 C_b(t) \\
\frac{dC_b}{dt} &= k'_3(t)C_f(t) - k_4 C_b(t) \\
k'_3(t) &= k_{on}\frac{B_{max} - \frac{C_b(t)}{SA}}{1 + D(t)} \\
D(t) &= B_1 \qquad (t<t_2) \\
&= B_2 + A \cdot \exp(-R(t - t_2)) \quad (t \geq t_2)
\end{aligned} \tag{3}$$

where $C_f$ and $C_b$ are the concentrations of radioactivity for free and specifically bound [$^{11}$C]raclopride in tissue, respectively; $B_{max}$ is the total dopamine $D_2$ receptor concentration; $k_{on}$ is the bimolecular association rate constant for raclopride; SA is the specific activity of administered [$^{11}$C]raclopride; $D$ is the concentration of free dopamine. In this simulation study, $t_2$ was set to 30 min, and SA that was decay corrected to the first injection time was assumed to be equal in first and second injections with a single synthesis. Each assumed parameter for $K_1$ to $k_4$ was obtained from our monkey study, and the $B_{max}$ value was as reported previously (Endres et al., 1997), thus $K_1 = 0.033$, $K_1/k_2 = 0.59$, $k_{on} = 0.0048$, $B_{max} = 17.6$; $k_4 = 0.026$; $B_1 = B_2 = 0$, and SA = 37 GBq/μmol at the time of first injection.

First, the magnitude of the $BP_{ND}$ change, derived from an increase in released dopamine, was investigated. Time–activity curves, including dopamine release, were simulated from Eq. (3), in which $A$ varied: 0.5, 1.0, 1.5 and 2.0, and $R$ varied: 0.04, 0.07, and 0.1. In these simulated TACs, $BP_{ND1}$ and $BP_{ND2}$ were estimated by the MI-SRTM, and the relationship between the magnitude of the BP reduction ($\Delta BP = (BP_{ND1} - BP_{ND2})/BP_{ND1}$) and the integral of the dopamine pulse $D$ in Eq. (3) was examined.

Next, the BP change caused by an increase in administered raclopride was investigated. $D(t)$ in Eq. (3) was set to 0, and tissue TACs were generated using the input plasma TAC in which administration of the first injection was assumed as 1 nmol raclopride, and the second injection was amplified from 1 to 50 times greater than the first injection. In these simulated TACs, $BP_{ND1}$ and $BP_{ND2}$ were estimated by the MI-SRTM, and the relationship between the magnitude of ΔBP and the amount of raclopride administered by the second injection was examined.

*Effect of binding change timing on $BP_{ND}$ estimates*

It is possible that the change in $BP_{ND}$ occurs either before, or after, the second injection of [$^{11}$C]raclopride. In the MI-SRTM, the error in the estimates for the first injection of [$^{11}$C]raclopride amplifies the errors in the estimates for the second injection. In this simulation, the effect of the onset of the dopamine pulse on the binding change of $BP_{ND}$, estimated by the MI-SRTM, was investigated using noiseless simulated TACs. First, TACs with a released dopamine pulse were generated using Eq. (3), with the parameters mentioned above, and three types of pulse ($A = 0.5$, $R = 0.1$; $A = 1.0$, $R = 0.07$; $A = 1.5$, $R = 0.04$) in which the onset time of the dopamine pulse, $t_2$ in Eq. (3), was changed from −10, −5, 0, 5, 10, 15 min against 30 min intervals of the second injection. The values for $BP_{ND1}$, $BP_{ND2}$, and ΔBP were estimated by the MI-SRTM, and the relationship between the onset time of the dopamine pulse and the $BP_{ND}$ estimates was investigated.

Next, TACs were generated by the SRTM with measured cerebellum TACs and assumed parameter values ($R_1 = 0.86$, $k_2 = 0.091$, and $BP_{ND1} = 2.2$) using the fourth-order Runge–Kutta method, assuming a prompt change of $BP_{ND}$ at −10, −5, 0, 5 and 10 min after the second injection (30 min intervals). The value of $BP_{ND2}$ was also varied so that ΔBP would be 0, 10, 20, 30, 40, 50, 60, 70, and 80%. In these simulated TACs, $BP_{ND1}$, $BP_{ND2}$, and ΔBP were estimated by the MI-SRTM, and the estimated values were compared with the true values.

*Effect of injection interval on $BP_{ND}$ estimates*

The relationship between the reliability of the $BP_{ND}$ estimates from the MI-SRTM and the injection interval was investigated with noise-added TACs. A dynamic tracer concentration for [$^{11}$C]raclopride was derived from the equation of MI-SRTM (Eq. (2)) with a measured cerebellum TAC used as the input function and the rate constant values given as true values ($R_1 = 0.95$, $k_2 = 0.067$, $BP_{ND1} = 2.6$, $BP_{ND2} = 2.6$, 1.8, or 0.78) assuming a prompt BP reduction at the time of the second injection. The timing of the second injection was varied from 20 min to 90 min after the first scan.

The Gaussian-distributed mean-zero noise with variance proportional to the true count was added to the non-decaying tissue activity for each frame using Eq. (4) (Logan et al., 2001):

$$\sigma_i(\%) = 100 \cdot F / \sqrt{C_t(t_i) \cdot e^{-\lambda t_i} \cdot \Delta t_i} \tag{4}$$

where $i$ is the frame number; $C_t$ is the non-decaying tissue radioactivity concentration derived from the rate constants and the input function; $t_i$ is the midpoint time of the $i$'th frame; $\Delta t_i$ is the data collection time; λ is the radioisotope decay constant; $F$ is a scaling factor representing the sensitivity of the measurement system, introduced here to adjust the noise level. It should be noted that this equation assumes that noise, which is added to the TAC, is determined by the count of the curve itself. In fact, noise is determined by the total counts in the slice, and is affected by random counts, dead time, etc. In this simulation study, $F$ was set to 15.0 so that the noise level would be the same as the noise level for regions of interest (ROI)-based analysis, and 1000 noisy data sets were generated for each injection interval.

In these simulated TACs, $BP_{ND1}$ and $BP_{ND2}$ were estimated by the MI-SRTM, and estimated $BP_{ND1}$, $BP_{ND2}$, and ΔBP values were compared with the true values. Parameter estimates were considered outliers if either $BP_{ND1}$ or $BP_{ND2}$ was outside the range $0.0 < BP_{ND} < 10.0$. The reliability of the estimated parameters was evaluated by the mean and coefficient of variation (COV; SD/mean[%]) of the estimates excluding outliers, and the relationship between the reliability of the parameter estimates and the injection interval was investigated.

*Monkey study analysis*

Studies on monkeys with dual injections of [$^{11}$C]raclopride were performed to determine whether the present approach can estimate two identical $BP_{ND}$ values when there is no change in binding conditions during the scan, and whether this approach can detect a change in $BP_{ND}$ values when the binding conditions do change during the scan. The monkeys were maintained and handled in accordance with guidelines for animal research on Human Care and Use of Laboratory Animals (Rockville, National Institute of Health/Office for Protection from Research Risks, 1996). The study protocol was approved by the Subcommittee for Laboratory Animal Welfare of the National Cardiovascular Center.

First, PET studies were performed in four cynomolgus macaques (weight 3.6 ± 0.56 kg) by administering the same molar amount of [$^{11}$C]raclopride for the first and second injections (Table 1). Anesthesia was induced with ketamine (8.4 mg/kg, intramuscularly) and xylazine (1.7 mg/kg, intramuscularly) and maintained by intravenous propofol (6 mg/kg/h) and vecuronium (0.02 mg/kg/h) during the scan. Initially, 418 ± 111 MBq of [$^{11}$C]raclopride was administered by a bolus injection, and after 30 min, the same molar amount of [$^{11}$C] raclopride as for the first injection, was administered by a bolus

**Table 1**
Injection protocol in monkey studies with dual injections of [$^{11}$C]raclopride.

| | Subject | Specific activity at the time of first injection [GBq/μmol] | Injection interval [min] | First injection | | Second injection | |
|---|---|---|---|---|---|---|---|
| | | | | Injected mass [nmol] | Injected activity at the time of first injection [MBq] | Injected mass [nmol] | Injected activity at the time of second injection [MBq] |
| | #1 | 64.9 | 30 | 8.4 | 548 | | 198 |
| | #2 | 75.2 | 30 | 5.9 | 444 | | 160 |
| Exp. 1 | #3 | 29.3 | 30 | 13.6 | 399 | Same as first injection | 144 |
| | #4 | 39.7 | 30 | 7.1 | 280 | | 101 |
| | mean ± SD | 52.3 ± 21.4 | 30 | 8.8 ± 3.4 | 418 ± 111 | | 151 ± 39.9 |
| Exp. 2 | #5 | 22.6 | 30 | 3.3 | 73.3 | 30.7 | 249 |

Exp. 1: Dual injections with same mass of [$^{11}$C]raclopride.
Exp. 2: Dual injections with different mass of [$^{11}$C]raclopride.

injection. Data were acquired for 60 min (10 s × 18, 30 s × 6, 120 s × 7, 300 s × 2 for the first injection; 10 s × 18, 30 s × 6, 120 s × 7, 300 s × 2 for the second injection). The specific radioactivity was 52.3 ± 21.4 GBq/μmol at the time of the first injection.

Next, PET studies were performed on a cynomolgus macaque (weight 6.0 kg) with the administration of different molar amounts of [$^{11}$C]raclopride for the first and second injections by changing the volume of second injection with [$^{11}$C]raclopride which was synthesized before the first injection (Table 1). For the first injection, a bolus of 73.3 MBq of [$^{11}$C]raclopride, (3.3 nmol of raclopride) was administered, and after 30 min, 249 MBq at the time of the second injection (decay corrected 691MBq) of [$^{11}$C]raclopride (30.7 nmol of raclopride) was administered by bolus injection. The specific radioactivity was 23 GBq/μmol at the time of the first injection.

PET scans were performed using a PCA-2000A positron scanner (Toshiba Medical Systems Corporation, Tochigi, JAPAN) that provides 47 planes and a 16.2 cm axial field of view. A transmission scan with a 3-rod source of $^{68}$Ge–$^{68}$Ga was carried out for 20 min for attenuation correction before the administration of [$^{11}$C]raclopride. Radioactivity was measured in two-dimensional mode and the data were reconstructed by a filtered back-projection using a Gaussian filter (full width at half maximum is about 6.0 mm (Herzog et al., 2004)). VOIs were defined manually over the left and right striatum and cerebellum for PET images, and the radioactivity concentration in these regions was obtained. For each region, $R_{11}$, $k_{21}$, $BP_{ND1}$, $R_{12}$, $k_{22}$, and $BP_{ND2}$ were estimated by MI-SRTM. In addition, parametric images were generated, estimating each parameter voxel by voxel, using the MI-SRTM with the basis function method.

## Results

### *Detection of $BP_{ND}$ change with dual-injection*

Typical examples of simulated TACs in the dual-injection study with dopamine release are shown in Fig. 1. In the simulation studies, the magnitude of ΔBP, estimated by the MI-SRTM, was investigated in the two cases where the specific binding changed due to the released dopamine pulse or to an increase in administered raclopride. The magnitude of ΔBP increased as the integral of the dopamine pulse increased (Fig. 2A). To some extent there was a good linear correlation between the reduction in $BP_{ND}$ and the integral of the dopamine pulse ($Y = 2.0*X + 2.3$, $R^2 = 0.95$ where $X < 15$ ($X$: Integral of the dopamine pulse, $Y$: reduction in $BP_{ND}$)); however the relationship did not remain linear for a large dopamine pulse. The reduction in $BP_{ND}$ also became greater when the injected mass of raclopride increased, although its relationship was nonlinear (Fig. 2B).

### *Effect of binding change timing on $BP_{ND}$ estimates*

In the simulation with a released dopamine pulse, when the dopamine pulse was released before the second injection, the $BP_{ND1}$ value was underestimated and $BP_{ND2}$ was overestimated, compared with the situation where the dopamine pulse was released at the same time as the second injection (Figs. 3A, B). On the other hand, when the dopamine pulse was released after the second injection, $BP_{ND1}$ was unchanged and $BP_{ND2}$ varied according to the onset and magnitude of the dopamine pulse. The reduction in $BP_{ND}$ also depended on the

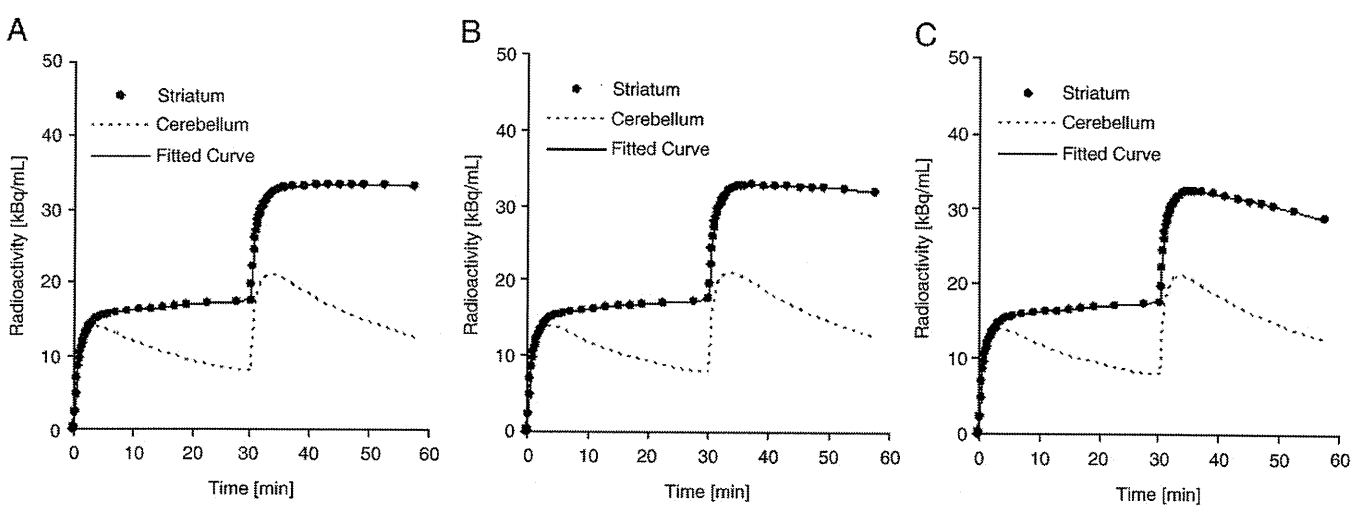


**Fig. 1.** Simulated time–activity curves for the striatum and cerebellum without dopamine pulse (A), with small dopamine pulse ($A = 0.5$, $R = 0.04$) (B), and with large dopamine pulse ($A = 1.5$, $R = 0.1$) (C), and fitted curve for the striatum by MI-SRTM.

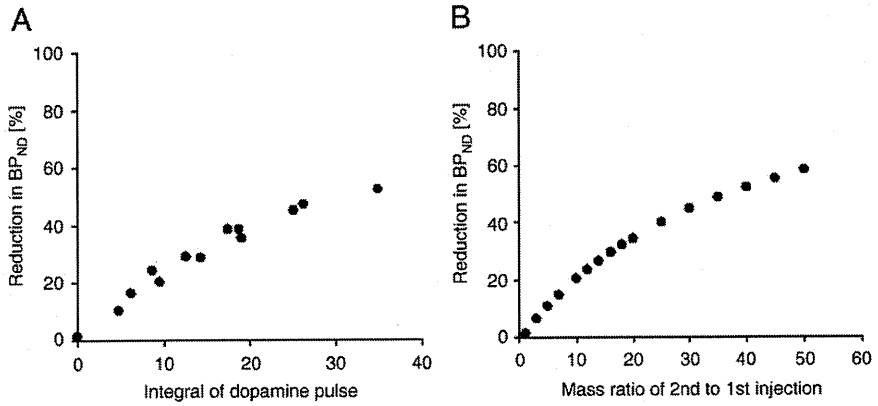


**Fig. 2.** Relationship between percentage reduction in $BP_{ND}$ and the integral of the dopamine pulse in simulation studies in which dopamine was released at the same time as the second injection, performed 30 min after first injection (A); and the relationship between percentage reduction in $BP_{ND}$ and the mass of the second injection in simulation studies in which a greater mass of raclopride was administered 30 min after the first injection.

onset, magnitude of amplitude, and decay rate of the dopamine pulse, and the reduction in $BP_{ND}$ was greatest when the dopamine pulse was released 5 min after the second injection (Fig. 3C). When the magnitude of the dopamine pulse was small, the detected $BP_{ND}$ reduction was small when the dopamine pulse was released before the second injection, becoming greatest (about 20%) when the pulse was released 5 min or 10 min after the second injection. When the magnitude of the pulse was medium, the $BP_{ND}$ reduction was 20% when the pulse was released 5 min before the second injection, and it was greatest (about 35%) when the pulse was released 5 min after the second injection. When the dopamine pulse was large, the detected $BP_{ND}$ reduction was 30% even when the pulse was released 10 min before the second injection, and was greatest (about 45%) when the pulse was released 0 or 5 min after the second injection.

In the simulation with prompt $BP_{ND}$ reduction, $BP_{ND1}$, $BP_{ND2}$ and ΔBP were estimated precisely by the MI-SRTM when the $BP_{ND}$ reduction occurred at 30 min, in other words, at the same time as the second injection (Fig. 4). In the case where the BP decreased before 30 min, the estimated $BP_{ND1}$ was lower than the true value for $BP_{ND1}$ (=2.2), and the magnitude of the underestimation increased when the true $BP_{ND2}$ was lower, that is to say, the reduction in $BP_{ND}$ was greater (Fig. 4A). There were slight errors in $BP_{ND2}$ estimates (Fig. 4B). When the $BP_{ND}$ decreased 50% ($BP_{ND1}=2.2$ and $BP_{ND2}=1.1$) at 10 min before the second injection, estimated $BP_{ND1}$ was 1.63 and $BP_{ND2}$ was 1.04. Conversely, when the BP decreased after 30 min, $BP_{ND1}$ was estimated precisely, and $BP_{ND2}$ was overestimated (Figs. 4A and B). The error in $BP_{ND2}$ estimates increased as the magnitude of the $BP_{ND}$ reduction increased. When the $BP_{ND}$ decreased 50% ($BP_{ND1}=2.2$ and $BP_{ND2}=1.1$) at 10 min after the second injection, estimated $BP_{ND1}$ was 2.20 and $BP_{ND2}$ was 1.28. With respect to the magnitude of the BP reduction, the estimated ΔBP was lower than the true value when the BP reduction was greater, or the difference between the timing of the $BP_{ND}$ decrease and the second injection was greater (Fig. 4C). When the $BP_{ND}$ reduction began 10 min before the second injection, the error in the estimated ΔBP was considerable. However, when the $BP_{ND}$ reduction began, either 5 min before or 5 min after, the second injection, the error in ΔBP was less than 5% when the reduction in the BP was lower than 50%.

### *Effect of injection interval on $BP_{ND}$ estimates*

Errors in the estimated $BP_{ND1}$, $BP_{ND2}$ and ΔBP values were investigated in simulated noise-added TACs for various injection intervals, and it was observed that the errors became larger as the injection interval became shorter (Fig. 5). The COVs of $BP_{ND1}$ and $BP_{ND2}$ were less than 5% and the bias was less than 1% when the injection interval was longer than 30 min, in both cases where the reduction in the $BP_{ND}$ was 30% and 70%. When ΔBP was 30%, the bias increased suddenly, and the COV of ΔBP rose to over 10% for an injection interval of less than 40 min. There were no outliers even if the injection interval was 20 min. Meanwhile, when ΔBP was 70%, there was little bias and the COV of ΔBP was less than 10% for an injection interval longer than 30 min. The COV of ΔBP in the 70% reduction TAC was lower than that in 30% reduction TAC. However,

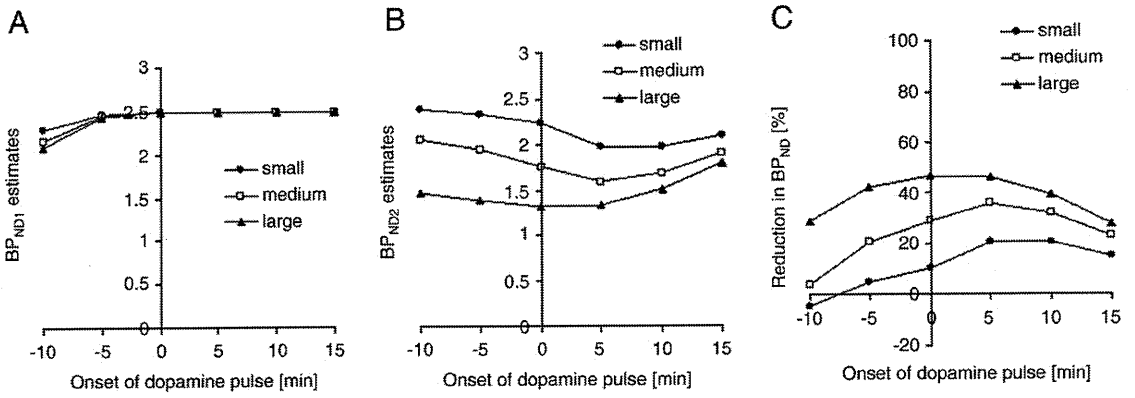


**Fig. 3.** Relationship between estimated values of $BP_{ND1}$ (A), $BP_{ND2}$ (B), reduction in $BP_{ND}$ (C) and the onset of the dopamine pulse, in simulation studies with a small pulse ($H=0.5$, $R=0.1$), medium pulse ($H=1.0$, $R=0.07$), and large pulse ($H=1.5$, $R=0.04$) released −10, −5, 0, +5, +10, or +15 min with respect to the second injection.

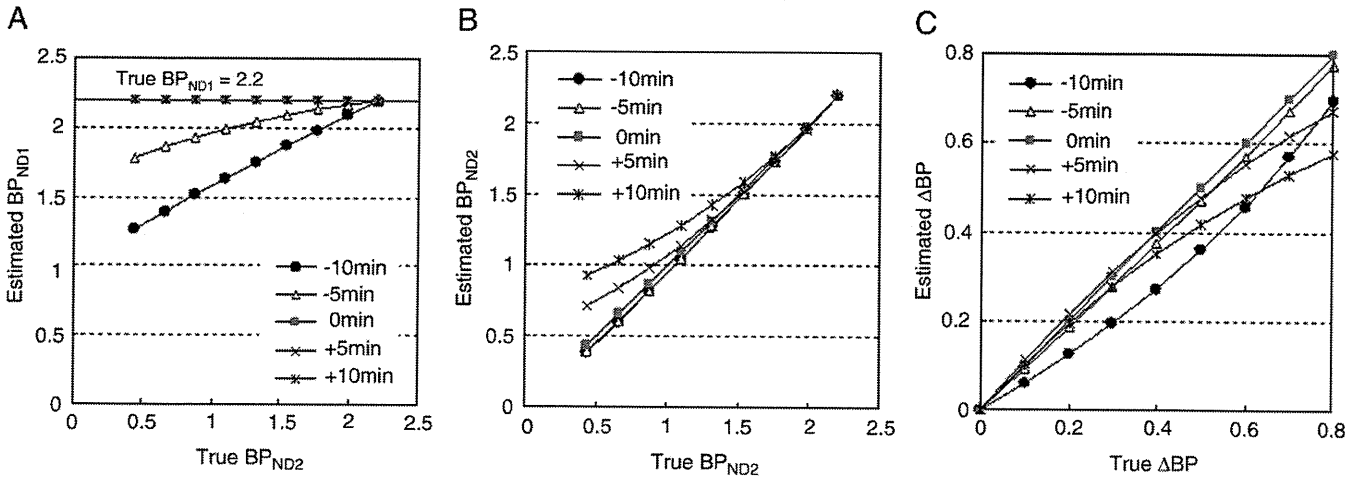


**Fig. 4.** Relationship between estimated values of $BP_{ND1}$ (A), and $BP_{ND2}$ (B) and the true values of $BP_{ND2}$, and the relationship between the estimated reduction in $BP_{ND}$ (ΔBP) and true ΔBP (C) in the simulation studies in which $BP_{ND}$ changed promptly from 2.2 to the true $BP_{ND2}$ at −10, −5, 0, +5, or +10 min, with respect to the second injection.

there were 22 outliers with unreasonable estimates when the injection interval was 20 min and one outlier in one thousand estimates when the injection interval was 30 min.

*Monkey studies*

Typical examples of TACs for the striatum and the cerebellum in the dual-injection study with the same amount of raclopride are shown in Fig. 6. In these studies, the $BP_{ND}$ values for the first and second injections could be estimated, and there were little differences between $BP_{ND1}$ and $BP_{ND2}$ (Table 2).

Time–activity curves for the striatum and the cerebellum in the dual-injection study using different amounts of raclopride are shown in Fig. 7, and the parametric images of $BP_{ND1}$ and $BP_{ND2}$ are shown in Fig. 8. The estimated BP decreased when the binding changed at the second injection due to the addition of more raclopride than was

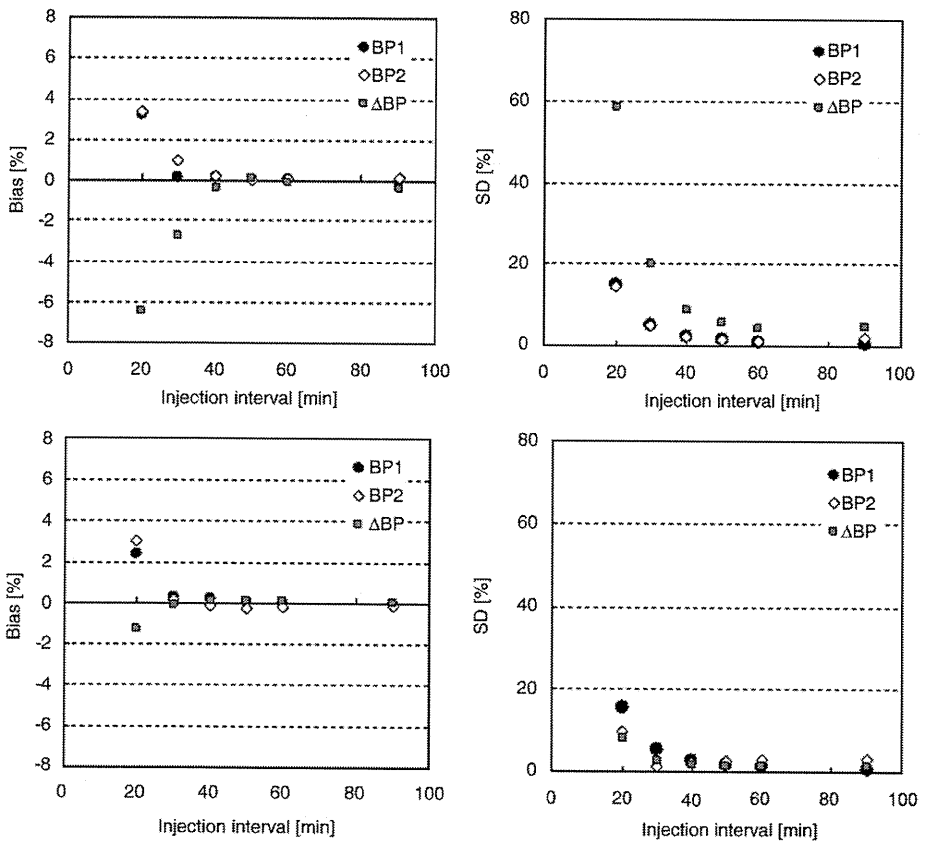


**Fig. 5.** Relationship between the injection interval and bias (left) or SD (right) of $BP_{ND1}$, $BP_{ND2}$, and the reduction in $BP_{ND}$ (ΔBP) when $BP_{ND}$ decreased by 30% (upper) or 70% (lower) at the time of second injection.

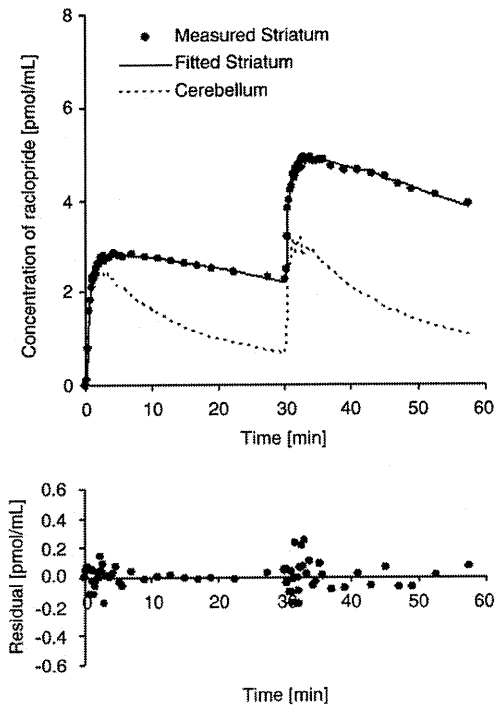


**Fig. 6.** Measured time–activity curves of the striatum and cerebellum in the dual-injection study with the same mass of [$^{11}$C]raclopride and a fitted curve for the striatum, using the multiple-injection SRTM (upper), and residuals between measured and fitted curves (lower).

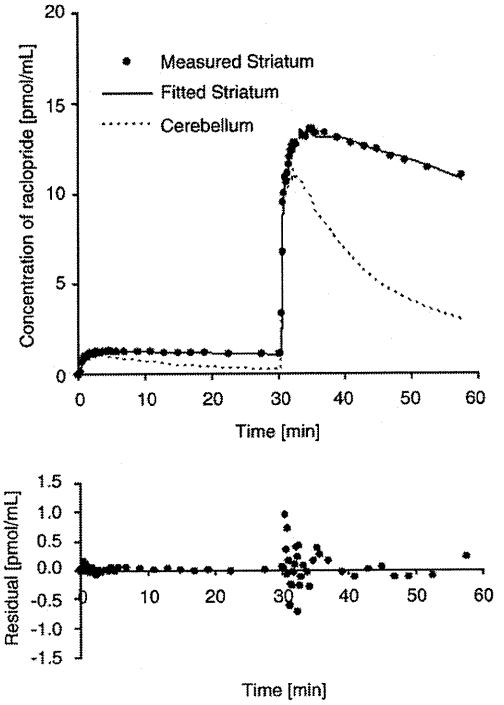


**Fig. 7.** Measured time–activity curves of the striatum and cerebellum in the dual-injection study with a different mass of [$^{11}$C]raclopride and a fitted curve for the striatum, using the multiple-injection SRTM (upper), and residuals between measured and fitted curves (lower).

administered for the first injection. Estimated $BP_{ND1}$, $BP_{ND2}$ and ΔBP values in the striatum were 2.7, 2.0, and 25%, respectively (Table 2). The reduction in $BP_{ND}$ was also observed in the parametric images as shown in Fig. 8.

## Discussion

In the competition paradigm, the binding potential of [$^{11}$C] raclopride reflects the condition of specific binding to dopamine $D_2$ receptors, which is affected by competition with other ligands if there are no changes in the density of the receptors. The SRTM can provide the $BP_{ND}$ value without invasive arterial blood sampling, using a TAC of the reference region, where specific bindings are negligible (Lammertsma and Hume, 1996), and this method has been widely used to estimate the binding of neuroreceptor ligands. However, in assessing temporal changes in the $BP_{ND}$ of the SRTM caused by competition for receptor binding due to pharmacological administration or cognitive activation, multiple [$^{11}$C]raclopride PET scans are necessary and a long study period is required. To overcome this complication, we have proposed a multiple-injection approach in which the temporal change in $BP_{ND}$ is quantified in a single scan with multiple [$^{11}$C]raclopride injections. This approach takes into account the residual radioactivity from the first injection in the target tissue, at the time of the second injection, as the initial condition in Eq. (2), and makes it possible to perform the second injection immediately, following data acquisition from the first injection. Thus it is possible to determine the change in $BP_{ND}$ from a short study period.

**Table 2**
Estimated $BP_{ND1}$, $BP_{ND2}$, and difference between $BP_{ND1}$ and $BP_{ND2}$ in monkey studies with dual injections of [$^{11}$C]raclopride.

| | Subject | $BP_{ND1}$ | $BP_{ND2}$ | ΔBP |
|---|---|---|---|---|
| | #1 | 1.86 | 2.15 | 0.15 |
| | #2 | 1.98 | 2.01 | 0.014 |
| Exp. 1 | #3 | 1.95 | 1.79 | −0.081 |
| | #4 | 2.33 | 2.39 | 0.027 |
| | mean ± SD | 2.03 ± 0.20 | 2.08 ± 0.25 | 0.029 ± 0.097 |
| Exp. 2 | #5 | 2.66 | 2.00 | −0.25 |

$\Delta BP = (BP_{ND2} - BP_{ND1}) / BP_{ND1}$.
Exp. 1: Dual injections with same mass of [$^{11}$C]raclopride.
Exp. 2: Dual injections with different mass of [$^{11}$C]raclopride.

There have been several investigators who attempted to perform multiple injections of ligands with PET studies for either obtaining receptor density and affinity by changing specific activity (Delforge et al., 1995; Millet et al., 1995; Morris et al., 1996a,b; Muzic et al., 1996; Christian et al., 2004; Gallezot et al., 2008), or obtaining different kinetic parameters simultaneously by injecting different tracers such as [$^{11}$C]flumazenil and [$^{18}$F]FDG (Ikoma et al., 2004; Koeppe et al., 2001). MI-SRTM gives us alternative approach for multiple-injection study which is aimed at shortening study period.

### *Detection of binding changes with the SRTM*

In the multiple-injection approach, it is assumed that the change in binding conditions is reflected by a reduction in $BP_{ND}$ estimated from the SRTM. The analysis method based on the compartment model assumes that the rate constants of $K_1$ to $k_4$ are constant during the scan. However, in studies with changes in binding conditions, levels of endogenous dopamine change after exposure to stimuli such as an amphetamine challenge (Endres et al., 1997; Laruelle et al., 1997), and the value of $k_3'(t)$ in Eq. (3) varies according to the concentration of free dopamine (Laruelle et al., 1997, Endres et al., 1997). Therefore, estimates of $BP_{ND}$ following exposure to stimuli are considered to be an average value over time that is influenced by the dynamics of the neurotransmitter. However, it has been reported that reductions in $BP_{ND}$, estimated from graphical analysis or multilinear analysis, in simulation studies for two separate bolus-injection scans, are related to the integral of dopamine release (Endres and Carson, 1998; Yoder et al., 2004), and the reduction in $BP_{ND}$ is a useful index for the evaluation of binding conditions in competition paradigms.

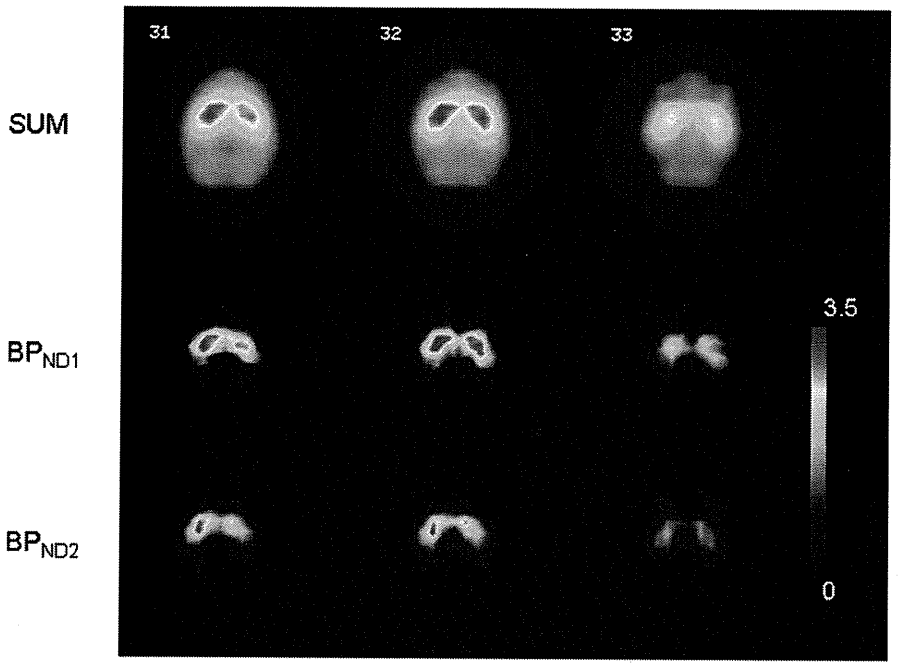


**Fig. 8.** Summation image and parametric images of $BP_{ND1}$ and $BP_{ND2}$ in the monkey study with dual injections of different masses of [$^{11}$C]raclopride.

In addition, in the SRTM, there are further assumptions that the target tissue and reference tissue can be expressed by a one-tissue compartment model, and the ratio of $K_1$ and $k_2$ are equal between the target and reference regions (Lammertsma and Hume, 1996). Strictly speaking, this assumption does not apply to [$^{11}$C]raclopride studies because significantly better fits were obtained with a two-tissue compartment model, as compared with those obtained with a one-tissue compartment model in cerebellum and striatum TACs (Lammertsma et al., 1996). Therefore, this assumption of the SRTM induces a bias in $BP_{ND}$ estimates even in an ordinary single-injection study. In the MI-SRTM, which is an extension of the SRTM, the effect of the assumption could be more severe than for the SRTM because the bias in $BP_{ND1}$ could be propagated to the estimation of $BP_{ND2}$. However, in our simulation studies, the $\Delta BP_{ND}$, estimated from the MI-SRTM, increased according to the increase in the dopamine pulse or to administered raclopride (Fig. 2). When the specific binding of administered [$^{11}$C]raclopride competed with that of endogenous dopamine, to some extent the reduction in BP increased in proportion to the integral of the released dopamine pulse, and approached saturation as the integral of the pulse increased. This is consistent with results reported in previous studies (Endres and Carson, 1998, Yoder et al., 2004). Furthermore, in the monkey studies, it was confirmed that there was little change in $BP_{ND}$ when the same mass of raclopride was administered for the first and second injections (Fig. 6), and the $BP_{ND}$ decreased in accordance with the increase in administered raclopride (Figs. 7 and 8). Morris et al. (1996b) intensively investigated the characteristics of multiple injections PET studies, and they showed varied specific activity by multiple injections introduced bias in estimates of kinetic parameters. Our results may be influenced by the abrupt discontinuity in mass of raclopride due to the second injection. However, the result of second monkey study (10 times higher mass in the second injection) agreed well with the simulation (Fig. 2B) although further validation studies will be needed to confirm this result.

*Effect of binding change timing on $BP_{ND}$ estimates*

In estimating the $BP_{ND}$ after the dopamine pulse release, the timing of the [$^{11}$C]raclopride injection has been shown to affect the $BP_{ND}$ estimates (Yoder et al., 2004). In the simulation study of our multiple-injection approach, $BP_{ND1}$ (in other words, the $BP_{ND}$ for the condition without dopamine activation) had few errors, except when the dopamine pulse was released 10 min before the second injection. In these simulations, $BP_{ND1}$ was estimated using the data from the time interval between the first injection and the second injection. Therefore, when the $BP_{ND}$ reduction, due to an increase in free dopamine, started before the second injection, the value for $BP_{ND1}$ was underestimated. However, this underestimation can be avoided by adjusting the data points used for the fitting of $BP_{ND1}$ so that $BP_{ND1}$ is determined before a change in the binding conditions. On the other hand, $BP_{ND2}$, (that is to say, the $BP_{ND}$ of the condition with dopamine activation) was affected by the timing of the dopamine pulse release. The estimated $BP_{ND2}$ decreased as the onset of the dopamine pulse occurred later, and was smallest when the dopamine pulse was released 5 min after the second injection. As a result, the magnitude of $\Delta BP$ was greatest when the dopamine pulse was released 5 min after the second injection.

The value of $k_3'(t)$ in Eq. (3) depends upon the amount of free dopamine at time $t$ (Endres et al., 1997, Endres and Carson, 1998) and the released dopamine pulse decreases as time goes by. Therefore, if the specific activity of administered [$^{11}$C]raclopride is high enough, the time-varying binding potential ($BPs(t) = k_3'(t)/k_4$) is lowest at the time of the pulse release, and it becomes greater, and approaches the level before the pulse release, as time passes. Meanwhile, the reduction in $BP_{ND}$ is determined by both the $BPs(t)$ and the concentration of free tracer (Endres and Carson, 1998). In the TACs from our simulation studies, the concentration of free [$^{11}$C]raclopride had a peak at about 5 min after the injection, and $\Delta BP_{ND}$ was greatest when the onset of the dopamine pulse occurred 5 min after the injection, as shown in Fig. 3C. Therefore, the reduction in $BP_{ND}$ was greatly affected, not only by the magnitude of the dopamine pulse, but also by its timing. In other words, if the kinetics of the free tracer are similar, that is to say the value of $k_2$ does not change markedly, and the timing of the dopamine release is the same, the estimated $\Delta BP$ changes according to the integral of the dopamine pulse as shown in Fig. 2.

In the situation where $BP_{ND}$ changed promptly, the $\Delta BP_{ND}$ also depends upon the magnitude and timing of the $BP_{ND}$ reduction. However, when $\Delta BP_{ND}$ was less than 40% and the time difference

between the binding change and second injection was within 5 min, the effect of the timing of the $BP_{ND}$ reduction was slight.

*Interval between the dual injections*

In the simulation study with noise for the ROI-based estimation, a dual-injection scan with a 30 min injection interval, gave unbiased and reliable $BP_{ND1}$ and $BP_{ND2}$ estimates (Fig. 5). In the 70% reduction TAC, the COV of $\Delta BP_{ND}$ was less than 5% when the injection interval was 30 min. Conversely, results from the 30% reduction TAC showed that a 50 min interval would be required to estimate $\Delta BP_{ND}$ within a 5% COV. In this study, we evaluated the reliability of $BP_{ND}$ estimates for an ROI-based estimation. However, in voxel-based estimations, the noise level is usually higher, so the COV of estimates can be expected to increase.

In the ROI analysis of human study with single injection, it is reported that a 30 min scan of [$^{11}$C]raclopride gave unbiased and reliable $BP_{ND}$ estimates (Ikoma et al., 2008). The kinetics of [$^{11}$C] raclopride in the human brain is different from that in the monkey brain, inducing the difference in required scan durations. The required injection interval for a reliable estimation depends on the kinetics of the ligand, the magnitude of $\Delta BP_{ND}$ and the noise level according to injection dose, ROI size, sensitivity of the measurement system, and so on. Therefore, evaluating the effect of the injection interval on the reliability of parameter estimates is important.

*Monkey studies*

In the simulation studies, it was demonstrated that the MI-SRTM approach could detect a change in $BP_{ND}$ caused by the release of a dopamine pulse or by the increase in administered raclopride. Furthermore, we demonstrated the validity of the proposed method using actual data from monkeys. As a result, the estimated $BP_{ND}$ reduction changed according to the injected mass of raclopride in the second injection, and this is consistent with the results from the simulation studies. We are planning further studies on monkeys with co-injection of various amount of cold raclopride to examine the relationship between the observed changes in $BP_{ND}$ and the occupancy of receptors. Furthermore, using the present approach, it may be possible to estimate endogenous dopamine release by pharmaceutical stimuli although the interpretation of the results must be made with caution because the level of endogenous dopamine is sensitive to the timing and the response of pharmaceutical manipulation (Yoder et al., 2004).

*Potential of the multiple-injection approach*

The dual-injection approach is able to assess the change in $BP_{ND}$ for receptor competition studies in a single PET scan and shortened study period, as compared to a conventional approach. However, this approach requires some caution. Firstly, the error due to residual radioactivity at the time of the second injection may affect the reliability of $BP_{ND2}$ estimates. Therefore, we estimated the residual radioactivity, not from the measured TAC, but from a fitted TAC from the first injection. In the simulation study, with noise-added TACs, the bias and COV of $BP_{ND2}$ estimated from the second injection were acceptable (Fig. 5).

Secondly, the administered molar amount of second injection must be same as that of the first injection for the evaluation of dopamine release, because the value of $BP_{ND}$ decreases according to the increase in administered raclopride even if the dopamine pulse does not be released (Fig. 2B). In addition, in the dual-injection study, the radioligand for the first injection remains in the tissue at the time of second injection. Therefore, the molar amount of administered raclopride needs to be sufficiently small, that is to say, the specific activity of administered [$^{11}$C]raclopride should be high enough. The mass of first injection is required to be less than about 1 nmol/kg so that the remained raclopride at the second injection does not affect $BP_{ND2}$ estimates (data not shown). To keep the amount of administered raclopride below 1 nmol/kg with the administration of 37MBq/kg [$^{11}$C]raclopride, its specific activity should be greater than 37 GBq/μmol. However, in the multiple-injection study, if one can synthesize [$^{11}$C]raclopride with high specific activity, it is an advantage that [$^{11}$C] raclopride, synthesized once before the scan, can be administered for both the first and second injections.

Thirdly, the timing of the second injection affected the $BP_{ND}$ estimates, as it was also observed in the estimations using two separate conventional scans. The timing of the second injection should be fixed within the intersubjects of the group, and the interpretation of the $\Delta BP_{ND}$ requires some caution when a time–activity curve of free [$^{11}$C]raclopride differs. The competition paradigm also should be applied carefully in case where the dopamine released slowly in response to stimuli, because it is often difficult to estimate the timing of the dopamine peak. Despite this, we have shown that the multiple-injection approach can be used to determine a reduction in $BP_{ND}$ values as effectively as using two separate scans, but within a single scan lasting 100 min.

The ESRTM approach can also provide $\Delta BP_{ND}$ values from a single-session scan by administering [$^{11}$C]raclopride using a bolus-plus-continuous (B/I) infusion approach (Zhou et al., 2006). Meanwhile, with the MI-SRTM approach, [$^{11}$C]raclopride can be administered several times by bolus injection, so there is no need to control the administered dose continuously, and it is easy to change the administered mass of raclopride significantly during the scan.

Since the MI-SRTM is a successor of SRTM, one advantage of the MI-SRTM is that the $BP_{ND}$ parametric map can be obtained as shown in Fig. 8, which is crucial to perform statistical parametric mapping (SPM) type analysis. The results of our simulation and monkey studies suggest that the MI-SRTM can be applied to the estimation of $\Delta BP_{ND}$ for human study, though the optimal injection protocol needs to be evaluated. One application of the MI-SRTM approach for the human study is to estimate occupancy within short period. By the MI-SRTM approach, one can estimate the $BP_{ND}$ value without antipsychotics and $BP_{ND}$ with antipsychotics from one session of PET study. This approach is also useful in the estimation of receptor density ($B_{max}$) and affinity ($K_d$) that normally requires several scans with variable masses of raclopride injections (Farde et al., 1986; Doudet et al., 2003). Furthermore, this approach can be applied to other PET ligands if the $BP_{ND}$ can be estimated by the SRTM approach.

In summary, we have developed a method for estimating the change in binding potential in a single PET scan using multiple injections of [$^{11}$C]raclopride and a simplified reference tissue model. Our simulations showed that the reduction in $BP_{ND}$, estimated by this approach, was related to the amount of released dopamine or to the administered mass of raclopride. We also demonstrated that the reduction in $BP_{ND}$ varied according to the increase in administered raclopride in monkey studies. The proposed method, with multiple injections, has potential for use in quantitatively assessing the change in specific binding, in a short study period, for several neurotransmitter competition studies.

## Acknowledgments

This research was supported by the Ministry of Education, Culture, Sports, Science and Technology, Grant-in-Aid for Young Scientists (B) (No.20790839), Japan, Kobe Cluster I and II, Ministry of Education, Culture, Sports, Science and Technology of Japan (MEXT; T.H.), and the MHLW (Ministry of Health, Labour and Welfare of Japan) Health Science Research Grant, H17-025 (T.H., H.I).

We are grateful to members of the Department of Investigative Radiology, National Cardiovascular Center Research Institute, for their support of the PET experiment and for helpful suggestions.

## Appendix A

The multiple-injection simplified reference tissue model is based on the following differential equations of the simplified reference tissue model on the assumption that the time–activity curves of the target and reference tissues can be fitted to a single tissue compartment model with plasma input (Lammertsma and Hume, 1996)

$$\frac{dC_t}{dt} = K_1 C_p(t) - k_{2a} C_t(t) \tag{A1}$$

$$\frac{dC_r}{dt} = K_1^r C_p(t) - k_2^r C_t(t) \tag{A2}$$

$$K_1 / k_{2a} = K_1 / k_2 \cdot (1 + \mathrm{BP_{ND}}) \tag{A3}$$

where $C_p$ is the metabolite corrected plasma concentration, $C_t$ and $C_r$ are the concentration in target and reference tissue, respectively, $k_{2a}$ ($\mathrm{min}^{-1}$) is the apparent (overall) rate constant for transfer from specific compartment to plasma in the target tissue.

Eqs. (A1) and (A2) are expressed as follows by Laplace transform:

$$sC_t(s) - C_t(0) = K_1 C_p(s) - k_{2a} C_t(s) \tag{A4}$$

$$sC_r(s) - C_r(0) = K_1^r C_p(s) - k_2^r C_t(s) \tag{A5}$$

where $C_t(0)$ and $C_r(0)$ are the total concentration in target and reference tissue, respectively, at the time of injection.

From Eqs. (A4),(A5) and the assumption $K_1^r / k_2^r = K_1 / k_2$, the following expression can be derived:

$$C_t(s) = R_1 C_r(s) + \frac{1}{s + k_{2a}}(k_2 - Rk_{2a}) C_r(s) + \frac{1}{s + k_{2a}}(C_t(0) - R_1 C_r(0)). \tag{A6}$$

From Eqs. (A3) and (A6), the following expression can be derived by inverse-Laplace transform:

$$C_t(t) = R_1 C_r(t) + \left(k_2 - \frac{R_1 k_2}{1 + \mathrm{BP_{ND}}}\right) e^{-\frac{k_2}{1 + \mathrm{BP_{ND}}} t} \otimes C_r(t) + (C_t(0) - R_1 C_r(0)) e^{-\frac{k_2}{1 + \mathrm{BP_{ND}}} t}. \tag{A7}$$

In the second injection, $R_1$, $k_2$, and $\mathrm{BP_{ND}}$ can be estimated by giving $C_t(t)$, $C_r(t)$, and $C_t(0)$ and $C_r(0)$ at the time of second injection. Meanwhile, in the first injection, $C_t(0)$ and $C_r(0)$ are 0 at the time of first injection, so $C_t(t)$ can be expressed as follows:

$$C_t(t) = R_1 C_r(t) + \left(k_2 - \frac{R_1 k_2}{1 + \mathrm{BP_{ND}}}\right) e^{-\frac{k_2}{1 + \mathrm{BP_{ND}}} t} \otimes C_r(t). \tag{A8}$$

## References


Breier, A., Su, T.P., Saunders, R., Carson, R.E., Kolachana, B.S., de Bartolomeis, A., Weinberger, D.R., Weisenfeld, N., Malhotra, A.K., Eckelman, W.C., Pickar, D., 1997. Schizophrenia is associated with elevated amphetamine-induced synaptic dopamine concentrations: evidence from a novel positron emission tomography method. Proc. Natl. Acad. Sci. U.S.A. 94, 2569–2574.

Carson, R.E., Breier, A., de Bartolomeis, A., Saunders, R.C., Su, T.P., Schmall, B., Der, M.G., Pickar, D., Eckelman, W.C., 1997. Quantification of amphetamine-induced changes in [$^{11}$C]raclopride binding with continuous infusion. J. Cereb. Blood Flow Metab. 17, 437–447.

Christian, B.T., Narayanan, T., Shi, B., Morris, E.D., Mantil, J., Mukherjee, J., 2004. Measuring the in vivo binding parameters of [18F]-fallypride in monkeys using a PET multiple-injection protocol. J. Cereb. Blood Flow Metab. 24, 309–322.

Delforge, J., Pappata, S., Millet, P., Samson, Y., Bendriem, B., Jobert, A., Crouzel, C., Syrota, A., 1995. Quantification of benzodiazepine receptors in human brain using PET, [$^{11}$C] flumazenil, and a single-experiment protocol. J. Cereb. Blood Flow Metab. 15, 284–300.

Doudet, D.J., Jivan, S., Holden, J.E., 2003. In vivo measurement of receptor density and affinity: comparison of the routine sequential method with a nonsequential method in studies of dopamine $D_2$ receptors with [$^{11}$C]raclopride. J. Cereb. Blood Flow Metab. 23, 280–284.

Endres, C.J., Kolachana, B.S., Saunders, R.C., Su, T., Weinberger, D., Breier, A., Eckelman, W.C., Carson, R.E., 1997. Kinetic modeling of [$^{11}$C]raclopride: combined PET-microdialysis studies. J. Cereb. Blood Flow Metab. 17, 932–942.

Endres, C.J., Carson, R.E., 1998. Assessment of dynamic neurotransmitter changes with bolus or infusion delivery of neuroreceptor ligands. J. Cereb. Blood Flow Metab. 18, 1196–1210.

Farde, L., Ehrin, E., Eriksson, L., Greitz, T., Hall, H., Hedstrom, C.G., Litton, J.E., Sedvall, G., et al., 1985. Substituted benzamides as ligands for visualization of dopamine receptor binding in the human brain by positron emission tomography. Proc. Natl. Acad. Sci. U.S.A. 82, 3863–3867.

Farde, L., Hall, H., Ehrin, E., Sedvall, G., 1986. Quantitative analysis of $D_2$ dopamine receptor binding in the living human brain by PET. Science 231, 258–261.

Gallezot, J.D., Bottlaender, M.A., Delforge, J., Valette, H., Saba, W., Dollé, F., Coulon, C.M., Ottaviani, M.P., Hinnen, F., Syrota, A., Grégoire, M.C., 2008. Quantification of cerebral nicotinic acetylcholine receptors by PET using 2-[$^{18}$F]fluoro-A-85380 and the multiinjection approach. J. Cereb. Blood Flow Metab. 28, 172–189.

Gunn, R.N., Lammertsma, A.A., Hume, S.P., Cunningham, V.J., 1997. Parametric imaging of ligand–receptor binding in PET using a simplified reference region model. Neuroimage 6, 279–287.

Hall, H., Köhler, C., Gawell, L., Farde, L., Sedvall, G., 1988. Raclopride, a new selective ligand for the dopamine-D2 receptors. Prog. Neuropsychopharmacol. Biol. Psychiatry 12, 559–568.

Herzog, H., Tellmann, L., Hocke, C., Pietrzyk, U., Casey, M.E., Kuwert, T., 2004. NEMA NU2-2001 guided performance evaluation of four Siemens ECAT PET scanners. IEEE Trans. on. Nucl. Science 51, 2662–2669.

Ikoma, Y., Toyama, H., Suhara, T., 2004. Simultaneous quantification of two brain functions with dual tracer injection in PET dynamic study. In: Iida, H., Shah, N.J., Hayashi, T., Watabe, H. (Eds.), Quantitation in Biomedical Imaging with PET and MRI. InElsevier, pp. 74–78.

Ikoma, Y., Ito, H., Arakawa, R., Okumura, M., Seki, C., Shidahara, M., Takahashi, H., Kimura, Y., Kanno, I., Suhara, T., 2008. Error analysis for PET measurement of dopamine $D_2$ receptor occupancy by antipsychotics with [$^{11}$C]raclopride and [$^{11}$C] FLB457. Neuroimage 42, 1285–1294.

Kim, K.M., Watabe, H., Hayashi, T., Hayashida, K., Katafuchi, T., Enomoto, N., Ogura, T., Shidahara, M., Takikawa, S., Eberl, S., Nakazawa, M., Iida, H., 2006. Quantitative mapping of basal and vasareactive cerebral blood flow using split-dose $^{123}$I-iodoamphetamine and single photon emission computed tomography. Neuroimage 33, 1126–1135.

Koepp, M.J., Gunn, R.N., Lawrence, A.D., Cunningham, V.J., Dagher, A., Jones, T., Brooks, D.J., Bench, C.J., Grasby, P.M., 1998. Evidence for striatal dopamine release during a video game. Nature 393, 266–268.

Koeppe, R.A., Raffel, D.M., Snyder, S.E., Ficaro, E.P., Kilbourn, M.R., Kuhl, D.E., 2001. Dual-[11C]tracer single-acquisition positron emission tomography studies. J. Cereb. Blood Flow Metab. 21, 1480–1492.

Köhler, C., Hall, H., Ogren, S.O., Gawell, L., 1985. Specific in vitro and in vivo binding of 3H-raclopride. A potent substituted benzamide drug with high affinity for dopamine D-2 receptors in the rat brain. Biochem. Pharmacol. 34, 2251–2259.

Lammertsma, A.A., Hume, S.P., 1996. Simplified reference tissue model for PET receptor studies. Neuroimage 4, 153–158.

Lammertsma, A.A., Bench, C.J., Hume, S.P., Osman, S., Gunn, K., Brooks, D.J., Frackowiak, R.S., 1996. Comparison of methods for analysis of clinical [$^{11}$C]raclopride studies. J. Cereb. Blood Flow Metab. 16, 42–52.

Laruelle, M., Iyer, R.N., al-Tikriti, M.S., Zea-Ponce, Y., Malison, R., Zoghbi, S.S., Baldwin, R.M., Kung, H.F., Charney, D.S., Hoffer, P.B., Innis, R.B., Bradberry, C.W., 1997. Microdialysis and SPECT measurements of amphetamine-induced dopamine release in nonhuman primates. Synapse 25, 1–14.

Logan, J., Fowler, J.S., Volkow, N.D., Ding, Y.S., Wang, G.J., Alexoff, D.L., 2001. A strategy for removing the bias in the graphical analysis method. J. Cereb. Blood Flow Metab. 21, 307–320.

Millet, P., Delforge, J., Mauguiere, F., Pappata, S., Cinotti, L., Frouin, V., Samson, Y., Bendriem, B., Syrota, A., 1995. Parameter and index images of benzodiazepine receptor concentration in the brain. J. Nucl. Med. 36, 1462–1471.

Mintun, M.A., Raichle, M.E., Kilbourn, M.R., Wooten, G.F., Welch, M.J., 1984. A quantitative model for the in vivo assessment of drug binding sites with positron emission tomography. Ann. Neurol. 15, 217–227.

Morris, E.D., Babich, J.W., Alpert, N.M., Bonab, A.A., Livni, E., Weise, S., Hsu, H., Christian, B.T., Madras, B.K., Fischman, A.J., 1996a. Quantification of dopamine transporter density in monkeys by dynamic PET imaging of multiple injections of $^{11}$C-CFT. Synapse 24, 262–272.

Morris, E.D., Alpert, N.M., Fischman, A.J., 1996b. Comparison of two compartmental models for describing receptor ligand kinetics and receptor availability in multiple injection PET studies. J. Cereb. Blood Flow. Metab. 16, 841–853.

Muzic, R.R., Nelson, A.D., Saidel, G.M., Miraldi, F., 1996. Optimal experiment design for PET quantification of receptor concentration. IEEE Trans. Med. Imaging 15, 2–12.

Yoder, K.K., Wang, C., Morris, E.D., 2004. Change in binding potential as a quantitative index of neurotransmitter release is highly sensitive to relative timing and kinetics of the tracer and the endogenous ligand. J. Nucl. Med. 45, 903–911.

Watabe, H., Endres, C.J., Breier, A., Schmall, B., Eckelman, W.C., Carson, R.E., 2000. Measurement of dopamine release with continuous infusion of [$^{11}$C]raclopride: optimization and signal-to-noise considerations. J. Nucl. Med. 41, 522–530.

Watabe, H., Ohta, Y., Teramoto, N., Miyake, Y., Kurokawa, M., Yamamoto, A., Ose, Y., Hayashi, T., Iida, H., 2006. A novel reference tissue approach for multiple injections of [C-11]Raclopride. Neuroimage 31 (Suppl. 2), T73.

Zhou, Y., Chen, M.K., Endres, C.J., Ye, W., Brasic, J.R., Alexander, M., Crabb, AH, Guilarte, TR, Wong, D.F., 2006. An extended simplified reference tissue model for the quantification of dynamic PET with amphetamine challenge. Neuroimage 33, 550–563.